NOVA SCHOOL OF SCIENCE & TECHNOLOGY

DEPARTAMENTO DE CIÊNCIAS DA VIDA

ANTÓNIO PICÃO DE ABREU CARVALHO

Licenciado em Bioquímica

TACKLING METASTASIS WITH GOLD NANOPARTICLES: INHIBITION OF INTERCELLULAR COMMUNICATION MEDIATED BY CANCER CELLS-DERIVED EXOSOMES

MESTRADO EM GENÉTICA MOLECULAR E BIOMEDICINA

Universidade NOVA de Lisboa

11, 2021

NOVA SCHOOL OF SCIENCE & TECHNOLOGY

DEPARTAMENTO DE CIÊNCIAS DA VIDA

TACKLING METASTASIS WITH GOLD NANOPARTICLES: INHIBITION OF INTERCELLULAR COMMUNICATION MEDIATED BY CANCER CELLS-DERIVED EXOSOMES

ANTÓNIO PICÃO DE ABREU CARVALHO
Licenciado em Bioquímica

Orientadora: Doutora Catarina Maria Roma Rodrigues, Pós-Doutorada da Faculdade de Ciências e Tecnologia da Universidade NOVA de Lisboa

Coorientador: Doutor Pedro Miguel Ribeiro Viana Baptista, Professor Catedrático da Faculdade de Ciências e Tecnologia da Universidade NOVA de Lisboa

Júri:

Presidente: Doutor Pedro Manuel Brôa Costa, Professor Auxiliar da Faculdade de Ciências e Tecnologia da Universidade NOVA de Lisboa

Arguente: Doutora Helena Luísa de Araújo Vieira, Professora Auxiliar da Faculdade de Ciências e Tecnologia da Universidade NOVA de Lisboa

Vogal: Doutora Catarina Maria Roma Rodrigues, Pós-Doutorada da Faculdade de Ciências e Tecnologia da Universidade NOVA de Lisboa

MESTRADO EM GENÉTICA MOLECULAR E BIOMEDICINA

Universidade NOVA de Lisboa
11, 2021

Tackling Metastasis with Gold Nanoparticles: Inhibition of Intercellular Communication Mediated by Cancer Cells-Derived Exosomes

ACKNOWLEDGEMENTS

Agradeço primeiramente a Deus o dom da vida, a misericórdia que tem tido para comigo e por me ter posto numa comunidade de iniciação cristã.

Agradeço à minha orientadora, Catarina, toda a paciência, a disponibilidade para me ajudar e o tempo que dispensou para me acompanhar, muitas vezes através de casa. Obrigado por sempre me ter posto à vontade e por tudo o que me ensinou. Agradeço também ao professor Pedro por ter sempre a porta do gabinete aberta para mim e por me encorajar a pensar fora da caixa. Agradeço à professora Alexandra, minha orientadora emprestada, que foi muito prestável desde o início ao fim. André, Rúben e Beatriz Costa, agradeço a boa disposição e o companheirismo. Vai também um grande obrigado à malta do lab, Sandra, Daniela, Margarida, Bilal, Beatriz Oliveira, pelas noitadas, a preparação dos reagentes, o ensino de novas técnicas e tudo mais. De uma forma geral, obrigado pela experiência que me proporcionaram, professores e colegas.

À minha família que me suporta e cuida sem cessar. Aos meus pais por tudo o que fizeram para eu chegar até aqui. Por todas as horas que passaste a cozinhar para eu não vir com a lancheira vazia para a Caparica mãe. Por todos as viagens que fizemos juntos pai. Nem dá para enumerar. Mariana, Isabel e Teresa por me aturarem em casa. Muito obrigado! Aos meus avós, que me dão tudo o que for preciso sem hesitar e que estão sempre presentes. À minha namorada, Teresita, como tem sido bom este tempo e como me tens ajudado! Tens sido um presente na minha vida. Obrigado Patrícia, minha companheira de laboratório e vida, por todas as conversas até tarde, as tostas na Teresa, sem ti não teria sido possível. Bernardo, sempre lá, contigo desabafo sobre tudo, já somos da família. Obrigado Carlota, fazemos a festa, é impossível sentir-me triste ao pé de ti. Pipe e Pipa, não há palavras, seremos sempre a família do Monte. Sem vocês não sei como tinha passado pelos tempos de faculdade. Isabel, obrigado por todos os passeios nas pausas da escrita da tese, todas as confidências e pela nossa amizade onde tantas vezes aparece Deus.

Agradeço por fim à Fundação para a Ciência e a Tecnologia, I.P., (FCT): UIDP/04378/2020 e UIDB/04378/2020 para UCIBIO; LA/P/0140/2020 para i4HB.

"Tu me cercaste por detrás e por diante, e puseste sobre mim a tua mão.
Tal ciência é para mim maravilhosíssima; tão alta que não a posso atingir"

Salmos 139,5-6

ABSTRACT

Metastases are accountable for at least 66.7% of cancer deaths, implying a terminal illness for the great majority of patients diagnosed with metastatic cancer. The last and rate-limiting step in invasion-metastasis cascade is colonization. Colonization is the process by which disseminated tumour cells penetrate distant tissues and adapt to the foreign "soil" in order to prosper. To hasten colonization, cancer cells often secrete soluble factors and extracellular vesicles such as exosomes through systemic circulation, which ultimately lead to creation of tumour permissive microenvironments at secondary organs, pre-metastatic niches. Exosomal integrins $\alpha_6\beta_1$ and $\alpha_6\beta_4$ secreted by MDA-MB-231 cells, a human breast cancer cell line, were found to specifically fuse with lung-resident fibroblasts and epithelial cells. The cargo release within recipient cells activates Src and upregulates pro-inflammatory *S100* genes, which generates lung pre-metastatic niches and promotes lung tropic metastasis. In this case, cell-cell communication via exosomes between primary tumour cells and microenvironment of distant organs is a key mediator of metastasis progression.

Taken into account the recent bet on antisense oligonucleotides therapeutics and the advent of nanotechnology, a gold-nanoconjugate with gene silencing activity was produced. This was achieved by functionalizing gold nanoparticles with an antisense oligonucleotide designed to silence *ITGA6*, the gene that encodes the α_6 subunit, present in integrins $\alpha_6\beta_1$ and $\alpha_6\beta_4$. The silencing efficacy was evaluated using MDA-MB-231 cells at the RNA and protein levels, and the existence of phenotypical changes between untreated and treated cells was assessed.

The nanoconjugate showed silencing activity. Reduced cellular levels of integrins $\alpha_6\beta_1$ and $\alpha_6\beta_4$ may lead to diminished packaging of these receptors into exosomes and impairment of integrin-mediated lung tropic metastasis. This nanoscale approach has potential to be employed to prevent lung metastasis, but further studies are required.

Keywords: metastasis, organotropism, breast cancer, exosomes, integrins $\alpha_6\beta_1$ and $\alpha_6\beta_4$, gold nanoparticles, antisense oligonucleotides

RESUMO

Pelo menos 66.7% das mortes por cancro são atribuídas à presença de metástases, implicando uma doença terminal para a grande maioria dos pacientes diagnosticados com cancro metastático. O passo limitante da cascata de invasão-metastização é o último passo, a colonização. A colonização é o processo pelo qual células tumorais disseminadas penetram tecidos distantes e se adaptam a "solo" desconhecido de modo a prosperar. Para acelerar o processo de colonização, as células cancerígenas libertam frequentemente fatores solúveis e vesículas extracelulares como os exossomas através da circulação sistémica, o que conduz à criação de microambientes permissivos ao desenvolvimento tumoral noutros órgãos, os nichos pré-metastáticos. Descobriu-se que as integrinas exossomais $\alpha_6\beta_1$ e $\alpha_6\beta_4$, libertadas por células do cancro da mama, se ligam especificamente a fibroblastos e células epiteliais residentes nos pulmões. A libertação do conteúdo exossomal nas células recetoras ativa a proteína Src e aumenta a expressão dos genes pro-inflamatórios *S100*. Esta interação leva à formação de nichos pré-metastáticos no pulmão e promove a metastização com tropismo para o pulmão. Neste caso, a comunicação célula-célula via exossomas entre o tumor primário e microambientes de órgãos distantes é o mediador chave da progressão metastática.

Tendo em conta a recente aposta nas terapêuticas de oligonucleótidos *antisense* e o advento da nanotecnologia, foi produzido um nanoconjugado de ouro com atividade de silenciamento génico. Isto foi alcançado através da funcionalização de nanopartículas de ouro com um oligonucleótido *antisense* desenhado para silenciar *ITGA6*, o gene que codifica para a subunidade α_6 das integrinas $\alpha_6\beta_1$ e $\alpha_6\beta_4$. A eficácia do silenciamento foi avaliada ao nível do RNA e da proteína usando células MDA-MB-231, e foi verificada também a existência de alterações fenotípicas entre células tratadas e não tratadas.

O nanoconjugado demonstrou atividade de silenciamento génico. A redução dos níveis de integrinas $\alpha_6\beta_1$ e $\alpha_6\beta_4$ pode levar à diminuição do empacotamento destes recetores nos exossomas e travar a metastização com tropismo para o pulmão mediada por integrinas. Esta estratégia à nanoescala tem potencial para ser utilizada para prevenir a metastização nos pulmões, mas são necessários mais estudos.

Palavras chave: metastização, organotropismo, cancro da mama, exossomas, integrinas $\alpha_6\beta_1$ e $\alpha_6\beta_4$, nanopartículas de ouro, oligonucleótidos *antisense*

TABLE OF CONTENTS

LIST OF FIGURES

LIST OF ABBREVIATIONS AND SYMBOLS

ASO
Antisense Oligonucleotide
ATTRv
Hereditary Amyloidogenic Transthyretin
Au-nanoconjugate
Gold Nanoconjugate
AuNP
Gold Nanoparticle
AuNP@PEG
Gold nanoparticle functionalized with polyethylene glycol
AuNP@PEG@ITGA6
Gold nanoparticle functionalized with polyethylene glycol and ASO designed to target *ITGA6* mRNA
Bax
Bcl-2-Associated X
BBB
Blood-Brain Barrier
Bcl-2
B-Cell Lymphoma 2
Bcl-xL
B-Cell Lymphoma-Extra Large
BM
Basement Membrane
BMDC
Bone Marrow-Derived Cell
CAFs
Cancer-Associated Fibroblasts
CNS
Central Nervous System
COX2
Cyclooxygenase 2
CSC
Cancer Stem Cell
CSF1
Colony Stimulating Factor 1
Ct
Threshold Cycle
CTC
Circulating Tumour Cell
DLS
Dynamic Light Scattering
DTC
Disseminated Tumour Cell
ECM
Extracellular Matrix
EE
Early Endosome
EGF
Epidermal Growth Factor
EMA
European Medicines Agency
EMT
Epithelial-Mesenchymal Transition
EPR
Enhanced Permeability and Retention
ER
Oestrogen Receptor
ESCRT
Endosomal Sorting Complex Required for Transport
E-selectin
Endothelial-selectin
EV
Extracellular Vesicle

FAK
Focal Adhesion Kinase
FAP
Familial Amyloid Polyneuropathy
FBS
Foetal Bovine Serum
FDA
Food and Drug Administration
HER2
Human Epidermal Growth Factor 2
IARC
International Agency for Research on Cancer
IGF
Insulin-Like Growth Factor
ILV
Intraluminal Vesicle
KLF
Krüppel-Like Factor
LSPR
Localized Surface Plasmon Resonance
MDSC
Myeloid-Derived Suppressor Cell
MIF
Migration Inhibitor Factor
miRNA
microRNA
MMPs
Matrix Metalloproteinases
mRNA
Messenger RNA
MVB
Multivesicular Body
NADPH
Nicotinamide Adenine Dinucleotide Phosphate
N-cadherin
Neuronal cadherin
NK cell
Natural Killer cell
PEG
Polyethylene Glycol
PBS
Phosphate Buffered Saline
PMN
Pre-metastatic Niche
PNS
Peripheral Nervous System
PR
Progesterone Receptor
pRB
Retinoblastoma Protein
Puma
p53 Upregulated Modulator of Apoptosis
RANKL
Receptor Activator of NF-κB Ligand
RNase H1
Ribonuclease H1
ROS
Reactive Oxygen Species
RTKs
Receptor Tyrosine Kinases
RT-qPCR
Quantitative Reverse Transcription Polymerase Chain Reaction
SDS-PAGE
Sodium Dodecyl Sulphate-Polyacrylamide Gel Electrophoresis
siRNA
small interfering RNA
SNARE
Soluble NSF Attachment Protein Receptor
SPC
Surfactant Protein C
TAM
Tumour-Associated Macrophage
TEM
Transendothelial Migration
TGFβ
Transforming Growth Factor β
TME
Tumour Microenvironment
UV-Vis
Ultraviolet-Visible

VEGF
Vascular Endothelial Growth Factor

VEGFR
VEGF Receptor

WHO
World Health Organization

ZO-1
Zonula Occludens-1

1. INTRODUCTION

1.1. Cancer Incidence and Mortality

According to the GLOBOCAN estimates[1], shared by the International Agency for Research on Cancer (IARC), a specialized cancer agency of the World Health Organization (WHO), in 2020, 19.3 million new cases of cancer were diagnosed and 10.0 million people died from the disease worldwide. The estimates also showed that the most incident type of cancer was breast cancer, accountable for 11.7% of the new cases, and the deadliest type was lung cancer, with 18.0% of all deaths. In 2019, cancer was the leading cause of death before the age of 70 years in 57 of the 185 countries analysed in the statistics[2]. Furthermore, European countries summed 22.8% of the new cancer cases and 19.6% of the cancer deaths, although it comprises only 9.7% of the world population[2]. Globally, approximately 1 out of 5 persons will develop cancer along their lifetime[3].

Regarding metastasis, a study carried out by Dillekås et al. revealed that 66.7% of all cancer deaths by solid tumours registered in Norway from 2005-2015 were caused by metastases[4]. However, the authors expose some suspicion about this number, believing that metachronous metastases (metastases discovered on advanced stage cancers) may be underreported, due to inaccurate registration of death certificates[4]. Clinical experience and some review articles[5,6] seem to indicate a higher percentage. Notwithstanding, these data sustain the idea that at least 66.7% of cancer deaths are caused by metastases[4]. Since metastatic disease is associated to worst outcome, it is imperative to expand our insights into the molecular mechanisms ruling cancer metastasis in order to restrain the burden of cancer.

1.2. Breast Cancer

As already mentioned, in 2020, breast cancer was the most common type of cancer worldwide, affecting 2.3 million people[1]. It was also the leading cause of death by cancer among women in the same year, taking 685 thousand lives[1]. On the other side, male breast cancer is a rare disease and statistics indicate that less than 1% of breast cancer patients are men[7]. Locoregional treatment (surgery and radiotherapy) and systemic therapy are the two main strategies employed to treat early breast cancer[8]. The adequate choice of systemic therapy relies mostly on immunohistochemical techniques to identify the molecular subtype[9]. Based on the presence or absence of molecular markers for oestrogen, progesterone and

human epidermal growth factor 2 receptors (ER/PR/HER2), breast cancer can be classified in hormone receptor-positive, HER2-positive and triple-negative[10]. Patients with hormone receptor-positive tumours receive endocrine therapy with or without chemotherapy, patients with HER2-positive tumours receive HER2-targeted therapy combined with chemotherapy, and patients with triple-negative tumours receive chemotherapy alone[10]. Approximately 6-10% of patients diagnosed with early breast cancer have metastatic disease at the time of diagnosis and around 30% of patients will eventually develop metastases[11]. While breast cancer detected at an earlier stage is considered curable, up to 70-80% of patients with stage IV breast cancer die of cancer in 5 years[12,13]. The main goal of treatment for metastatic breast cancer is usually prolongation of survival with minimal toxicity[14]. Current limitations of treatment for metastatic breast cancer comprise lack of known oncogenic drivers of the disease and occurrence of secondary resistance[15]. Two factors that contribute to therapeutic resistance are heterotypical interactions within the tumour microenvironment (TME) and the existence of a subpopulation of cancer stem cells (CSCs)[16].

1.3. Tumorigenesis

In 1953, Nordling consolidated a theory that offered an explanation for the appearance of cancer[17]. The theory was grounded on the assumption that cancer evolved from normal cells which accumulated diverse genetic lesions and were able to thrive. Later, in the 1970s, Cairns and Nowell highlighted the extraordinary resemblance between cancer development and the evolution of species described by Darwin[18,19]. Thus, the clonal evolution model (also termed stochastic model) emerged. According to this model, cancer arises as an evolutionary process that is driven by the occurrence of somatic cell mutations with sequential, subclonal selection and expansion of the fitter variants[20,21]. Tumorigenesis was understood as a slow, progressive, multistep disease[22,23].

The CSC model (also termed hierarchic model) came next supported by studies[24,25] as the one conducted by Bonnet and Dick[26]. It was explicit that in some tumours was possible to separate a fraction of cancer cells with indefinite potential for self-renewal and the ability of driving tumorigenesis *in vivo*[27–32]. At least two ways of causing the disordered outgrowth of CSCs were found. In the first, these cells arise through the incidence of oncogenic mutations in normal stem cells inactivating constraints on normal stem cell expansion[33,34]. In the second, oncogenic mutations empower transit-amplifying cells to continue to proliferate without entering a postmitotic differentiated state, therefore generating a pool of self-renewing cells[33,34]. Once formed, CSCs give rise to a diverse low-tumorigenic progeny[35]. It is argued that CSCs undergo epigenetic changes analogous to the differentiation of normal cells, creating a tumour constituted by cancer cells organized hierarchicaly[36–41]. Efforts have been made to target CSCs with some therapies being tested in patients[42]. The clonal evolution and CSC models are not mutually exclusive in cancers that fit in a stem cell model, since CSCs would be expected to evolve by clonal evolution[35].

Tumorigenesis is a highly complex and dynamic process. In the disease progression intervene a myriad of participants from the TME[43] and it was reported a relevant contribution from the cooperative behaviour of different subclones from within the tumour community as

well[44]. At the same time that multistep development of cancer takes place, tumours acquire some common features, which are detailed in the next subchapter.

1.4. Hallmarks of Cancer

At the turn of the century, Weinberg and Hanahan shed light on six biological capabilities associated with cancer development: sustaining proliferative signalling, evading growth suppressors, resisting cell death, enabling replicative immortality, inducing angiogenesis, and activating invasion and metastasis[6]. More than a decade later, they added another two emerging hallmarks: reprogramming of energy metabolism and evading immune destruction[45]. Alongside, they strengthen the idea that the driving forces behind the oncogenic phenotype are genome instability and tumour-promoting inflammation induced by cells from the immune system. To clarify how cancer cells deviate themselves from the normal route of cellular life and death, each of the traits mentioned are briefly explored below. Figure 1 summarizes the hallmarks of cancer.

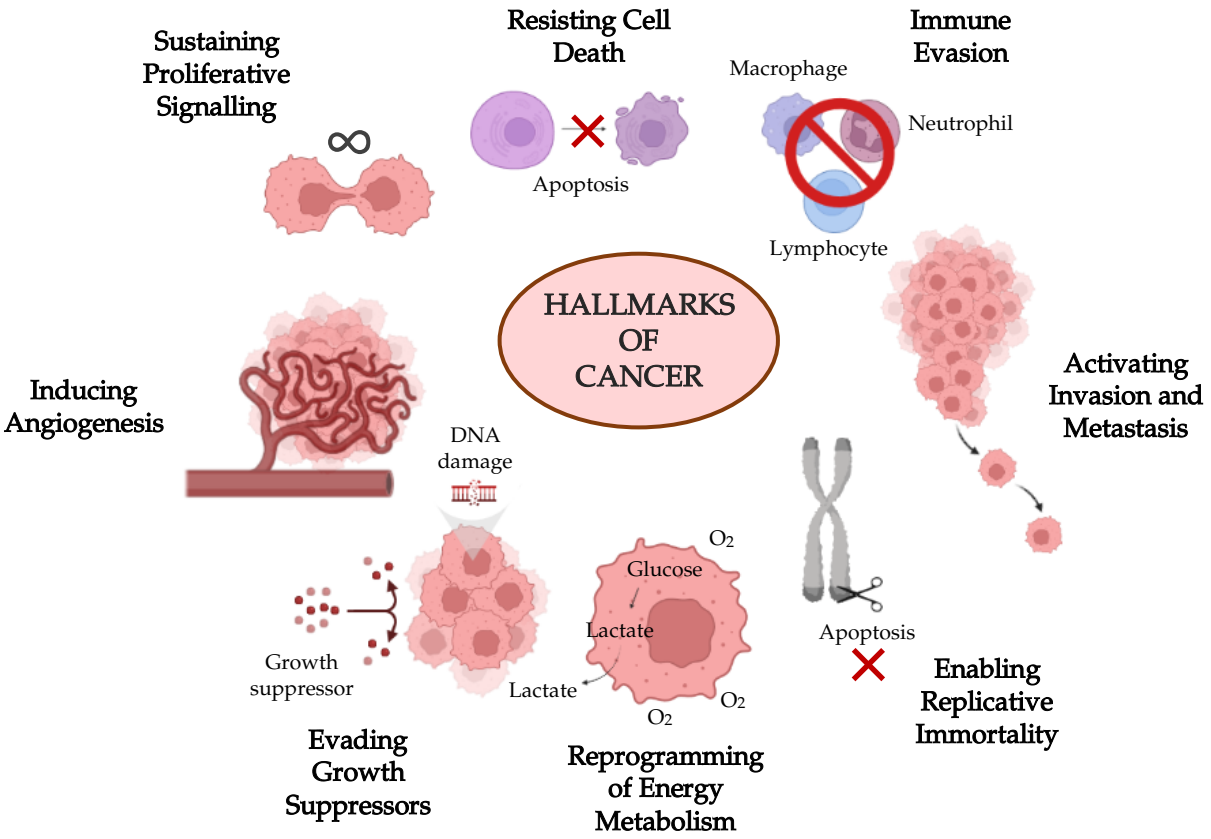

Figure 1. Schematics of the hallmarks of cancer progression. Created with BioRender.com.

1.4.1. Sustaining Proliferative Signalling

The ability of sustaining chronic proliferation is the most intuitive and common characteristic of cancer[46]. For the purpose of constitutively activating mitogenic signalling, cancer cells frequently increase the production and release of growth-promoting signals[47].

These signals, growth factors, bind to cell-surface receptors, such as receptor tyrosine kinases (RTKs), which are often overexpressed or overactivated in tumour cells. RTKs participate in intracellular signalling pathways that regulate cell cycle and growth and may influence other biological processes, such as cell survival and energy metabolism, giving tumour cells an advantage over the surrounding normal cells[45,48–52].

1.4.2. Evading Growth Suppressors

Cancer cells also develop the trait of avoiding the entrance in programs that negatively regulate cell proliferation. Many of these programs depend on tumour suppressor genes. The two canonical tumour suppressors genes encode pRB (retinoblastoma protein) and the p53. Cancer cells which succeed at attenuating the pRB pathway lose a critical gatekeeper of cell-cycle progression[45,53,54]. Alongside, p53 receives input from stress and abnormality sensors from inside the cell that are alert to excessive DNA damage[55,56] and, at the same time, to low levels of nucleotide pools, growth-promoting signals, glucose and oxygenation[45,57]. Thus, cancer cells often become insensitive to important checkpoint mechanisms that impede disordered replication.

1.4.3. Resisting Cell Death

Programmed cell death by apoptosis is a natural obstacle to tumorigenesis. The apoptotic machinery is triggered when cells are exposed to physiologic stress[58]. These machinery covers an upstream set of regulatory proteins, members of the B-cell lymphoma 2 (Bcl-2) family[58], initiator caspases (caspases 8 and 9) and downstream effector caspases[59]. There are two major pathways that lead to the activation of initiator caspases: extrinsic and intrinsic pathways[60]. Activation of apoptotic caspases generate a cascade of signalling events that permit the controlled demolition of cellular components, cell disassembly, cell death, and, ultimately, the phagocytosis and removal of the cell debris[61]. Tumour cells use various strategies to limit or circumvent apoptosis, being the most common the gaining of mutations in *TP53*, that result in loss of function of p53 tumour suppressor, the upregulation of antiapoptotic regulators [Bcl-2, B-cell lymphoma-extra large (Bcl-xL)] or survival signals [insulin-like growth factor (IGF)-1/2], the downregulation of proapoptotic factors [Bcl-2-associated X (Bax), Bim, p53 upregulated modulator of apoptosis (Puma)], or by inhibition of the extrinsic ligand-induced death pathway[45].

1.4.4. Enabling Replicative Immortality

Without enabling replicative immortality, cancer cells are kept arrested in the nonproliferative state of senescence or go through crisis (a stage characterized by multiple chromosomal abnormalities) accompanied by cell death[62,63]. In each round of replication, normal cells lose small DNA fragments due to the inability of DNA polymerase fully replicate chromosome ends (telomeres)[64]. Being high replicative frequency a known feature of tumour cells, this phenomenon eventually leads to critical deletions on coding regions triggering senescence or cell death[64]. In order to thwart this trend, cancer cells upregulate the expression of telomerase[65,66] or, less frequently, hasten an alternative recombination-based telomere maintenance mechanism[67].

1.4.5. Inducing Angiogenesis

Cancer cells largely depend on the free access to nutrients and oxygen, and from the possibility to discard waste products and carbon dioxide to sustain the uncontrolled growth and proliferation[45]. In this sense, the process of angiogenesis takes great relevance in fuelling the advance of tumour progression[68,69]. Angiogenesis is activated during embryonic development and only transiently during wound healing in adults[70]. Cancer cells, however, unveil the trail to operate the "angiogenic switch", which is induced by increasing the pro-angiogenic gene expression after sensing physiological stimuli, such as hypoxia, and also by oncogene activation or tumour suppressor gene mutation[71]. Vascular endothelial growth factor (VEGF) is the key mediator of angiogenesis in cancer, regularly upregulated by oncogene expression[68–72].

1.4.6. Reprogramming of Energy Metabolism

Altered metabolic patterns in cancer cells were reported in the 1920s by Warburg[73], when he noted that cultured tumour tissues had high rates of glycose uptake and lactate secretion even in aerobic conditions (aerobic glycolysis), phenomenon commonly termed Warburg effect[74]. Since then, it was recognized that tumours reprogram metabolism pathways to overcome issues like subsist in nutrient-poor environments[75–77]. Some of the metabolic changes orchestrated by malignant cells are the increased uptake of glucose and amino acids, the use of alternative modes of nutrient acquisition, the diversion of glycolysis/ tricarboxylic acid cycle intermediates for biosynthesis and nicotinamide adenine dinucleotide phosphate (NADPH) production, increased demand for nitrogen, alterations in metabolite-driven gene regulation (increased histone acetylation as a consequence of accumulation of cytosolic acetyl-CoA, as an example), and different metabolic interactions with the microenvironment[78].

1.4.7. Evading Immune Destruction

The roots of the immune surveillance concept were established in 1909 when Paul Ehrlich predicted that the immune system repressed the growth of carcinomas[79]. Later, Burnet and Thomas formally introduced a hypothesis stating that the immune system exerted protection against nascent cancers by destroying malignant cells before they developed into detectable tumors[80–83]. Nevertheless, they could not find experimental evidence to convincingly support this hypothesis at the time[84–87]. Subsequent studies led to the formulation of a broader hypothesis: cancer immunoediting[88]. Cancer immunoediting is constituted by three phases: elimination, equilibrium and escape[89]. In the first phase, transformed cells are eliminated by the competent immune system. In the second phase, tumour cells that manage to avoid immune destruction may then enter in a state of immune-mediated dormancy where editing takes place. In the third and final phase of the process, the immunologically shaped tumours begin to grow progressively and establish an immunosuppressive tumour microenvironment[90].

The capability of operating invasion and metastasis are presented more in-depth in the next subchapter.

1.5. Invasion and Metastasis

The formation of metastases is a multistep process that can be described by a succession of discrete events, termed the invasion-metastasis cascade[45,91–93]. The five key steps of the metastatic cascade include (1) invasion through the surrounding extracellular matrix (ECM) and stromal cell compartment, (2) intravasation into the lumina of blood vessels, (3) survival in circulation, (4) extravasation into the parenchyma of distant organs, and (5) colonization[94,95]. These events are in great part modulated by stromal and immune cells recruited to the TME[96].

The basement membrane (BM), a thin, dense sheet of ECM, functions as a structural barrier to cancer cell invasion, intravasation, and extravasation[97]. The expanding tumour mass must crack through the BM to invade adjacent tissues and migrate toward blood vessels[97]. The reactive stromal and immune cells can remodel the ECM via secretion of proteases, such as matrix metalloproteinases (MMPs), resulting in degradation of the BM[98–104]. Furthermore, in order to gain migratory and invasive properties, cancer cells exploit determinant mechanisms in embryonic development and tissue repair, such as the epithelial-mesenchymal transition (EMT)[105]. By passing from an epithelial to a mesenchymal state, cancer cells are endowed with motility, which can promote invasion to adjacent tissues and escape through the bloodstream[106].

Intravasation involves the passage of carcinoma cells through the endothelial cell barrier that forms the walls of blood and lymphatic vessels[107], transendothelial migration (TEM). Since hematogenous circulation is the principal mode of systemic tumour cell dissemination[5], the following approach to intravasation, circulation and extravasation topics focus on this type of dissemination. Intravasation can occur through invasion dependent and independent mechanisms[108]. Invasion independent intravasation arises when neoangiogenesis and vascular remodelling take place and cancer cells have access to leaky, malformed microvessels[107]. An invasion dependent mechanism entails chemotaxis via the colony stimulating factor 1/epidermal growth factor (CSF1/EGF) paracrine signalling between cancer cells and tumour-associated macrophages (TAMs)[108–110].

When migrating tumour cells or loose cells carried through the *de novo* vasculature reach the bloodstream, encounter a hostile environment with some obstacles to overcome: anoikis, hemodynamic forces and destruction by the immune cells[111]. The survival of circulating tumour cells (CTCs) and CTC clusters in its intravascular journey depends on the vessel size, shear stress and flow rate of the fluids[112]. High flow velocities and shear stress lead to cell cycle arrest, physical damage, necrosis and apoptosis[113,114]. In turn, intermediate flow velocities favour interactions with other blood-borne cells[113]. Natural killer (NK) cells may target and destroy CTCs by direct contact and lysis[113,115]. However, it was shown that, in association with platelets, the metastatic potential of CTCs administered on normal mice were higher comparatively to mice lacking a Gαq, a G protein critical for platelet activation[116]. When activated, platelets release granules containing growth factors, chemokines and proteases, which exert a pro-coagulant activity[111]. This event leads to the assembly of a network of activated platelets and fibrinogen around the CTCs that shield tumour cells from the NK cell activity, promotes the entrapment of other CTCs and the attachment to the endothelium[111,117].

Extravasation begin with attachment of CTCs or CTC clusters to endothelial walls, which can be achieved by occlusion-mediated arrest, but also through active cell adhesion[111]. Early attachment of cancer cells to endothelial cells can happen by the establishment of interactions between endothelial-selectin (E-selectin) and receptors displayed on the membrane of cancer cells, such as sialyl Lewis X/A glycoconjugates and CD44[111]. It was also demonstrated the occurrence of neuronal cadherin (N-cadherin) homophilic interactions between these cells[118]. Nonetheless, stable adhesion requires the binding of integrins and MUC1 to endothelial cells, in addition to CD44[111].

Metastatic colonization involves evading immune defences, surviving as latent tumour-initiating seeds, creating supportive niches and eventually overgrow[119]. The role of immunosuppression on the prevention of metastatic colonization was focused by studies as the one conducted by Smyth et al. that concluded that depletion of NK cells resulted in greater risk of developing metastasis in C57BL/6 (RM-1 prostate carcinoma) and BALB/c (DA3 mammary carcinoma) mice[120]. Additionally, RET.AAD mice (melanoma) lacking CD8+ T cells had more metastases than normal mice[121]. Thus, immune mechanisms are considered to be crucial in the protection against nascent micrometastases.

Upon infiltrating a target organ, disseminated tumour cells (DTCs) can undergo proliferative quiescence and enter a dormant state[122]. Dormancy can arise at a later stage due to insufficient vascularization or due to pressure exerted by the immune system, creating dormant micrometastases[119,123–126]. Metastasis reactivation seems to be associated to the acquisition of CSC characteristics and to the downregulation of EMT-inducers[122]. Moreover, DTCs must adapt to the foreign soil in order to prosper[119]. Malanchi et al. found that infiltrating tumour cells educate fibroblasts to produce and release periostin (a component of the ECM) in the secondary target organ (in this case lung) to initiate colonization[127]. Periostin is required for the lodging of CSCs, which in turn can populate the metastatic niche due to its self-renewal capabilities[127]. However, the alteration of local environments at secondary organs can occur even before arrival of DTCs, to create pre-metastatic niches (PMNs) [128].

1.5.1. Pre-metastatic Niche

In contrast to survival in circulation, adhesion to endothelial walls and extravasation, metastatic colonization is a highly inefficient process, emerging as a rate-limiting step in the metastatic cascade[95]. In this context, it is relevant to bring up the revolutionary thought of Stephen Paget, shared with the scientific community in 1889[129]. To his comprehension, like seeds that are carried by the wind in all directions but can only live and grow if they fall in congenial soil, CTCs do not contain the intrinsic potential of autonomously induce the growth of metastases but require, to a lower or higher extent, a predisposed or prepared "soil", the PMN[129]. Primary tumour cells lay fertile soil on other organs by long distance communication with tissue-resident cells, which promote local microenvironmental changes that facilitate the development and outgrowth of DTCs[130]. The agents operating these alterations are soluble factors and extracellular vesicles (EVs) such as exosomes, released in the systemic circulation by cancer cells[131–133].

1.6. Tumour Microenvironment

Cancers are heterogeneous cellular entities, whose growth and dissemination depends on reciprocal interactions between cancer and non-transformed cells[96,134–136]. How these non-transformed cells, leading figures in cancer metastasis, are recruited to the TME have been a matter of intense studying and it is known that inflammation is highly associated with the process[137,138]. Cancer cells that manage to usurp signalling pathways associated with proliferation, through oncogene mutations, frequently activate downstream pathways involved in inflammation[138]. The liberation of inflammatory mediators [such as chemokines, cytokines, prostaglandins and cyclooxygenase 2 (COX2)] leads to the recruitment and activation of various leukocytes, specially from the myeloid lineage[138]. The activated and mobilized myeloid cells start to produce further inflammatory cytokines that promote tumour cell cytokine-driven proliferation, recruit further immune and stromal cells, and incite an adaptive immune response[139]. Contrarily to wound healing, persisting oncogene-related stress and cell death drive to a feed-forward loop of inflammation-induced signalling and inflammatory cell attraction, reinforcing the primitive idea that tumours are like wounds that do not heal[140]. Beyond that, fibroblasts are recruited to assist cancer cells in the TME through a multitude of different mechanisms in addition to inflammatory modulation[141]. Cancer-associated fibroblasts (CAFs), in this way designated when activated by cancer cells, can be generated by physical changes in the ECM, the presence of RTK ligands or transforming growth factor β (TGFβ) family ligands, physiologic stress [reactive oxygen species (ROS) and unusual tumour-associated metabolites], and contact signalling (Notch and Eph-ephrins)[141].

1.7. Exosomes

Exosomes are a type of EV with size range of ~40 to 160 nm, formed in the endosomal network[142,143]. They can incorporate proteins, lipids, nucleic acids, metabolites, and aminoacids[142]. Exosomes allow intercellular communication and are associated with various biological processes, such as mammalian reproduction and development, immune responses, metabolic and cardiovascular disease, neurodegeneration and cancer[142]. Exosomes are currently recognized as fundamental mediators of the PMN formation and organ-specific metastasis[131].

1.7.1. Biogenesis and Secretion

Exosomes are generated in the endosomal pathway that starts by invagination of the plasma membrane, giving rise to early endosomes (EEs), and subsequent inward budding of EEs to form multivesicular bodies (MVBs) containing intraluminal vesicles (ILVs)[144]. Cargo clustering, and budding and fission of endosome membrane were reported to be executed by the endosomal sorting complex required for transport (ESCRT) machinery[145]. Alternative mechanisms exist, such as hydrolysis of neutral type II sphingomyelinase into ceramide on endosome membrane subdomains causing a negative curvature that stimulates vesicles generation[145]. As EEs mature into MVBs, they accumulate ILVs in their lumen[146]. Membrane traffic is regulated by the Rab family of small GTPases (Figure 2)[147,148]. Likewise, various Rab GTPases mediate the movement of vesicles and multivesicular compartments through the

cytoskeletal and microtubule network[149]. RAB5 governs transportation of endocytic vesicles to EEs and maturation of EEs into MVBs[146]. Distinctively, the targeting of MVBs to lysosome for degradation relies on the action of RAB7[145]. RAB11 and RAB35 are linked to secretion of ILVs from the early or recycling endosomes to the extracellular milieu[146,150]. Finally, RAB11, RAB35, RAB27a and RAB27b promote secretion of ILVs from MVBs to the extracellular space, then designated exosomes[146,150]. The release of exosomes requires association with fusion machinery, such as soluble NSF attachment protein receptors (SNAREs) and tethering factors at the cell membrane[151].

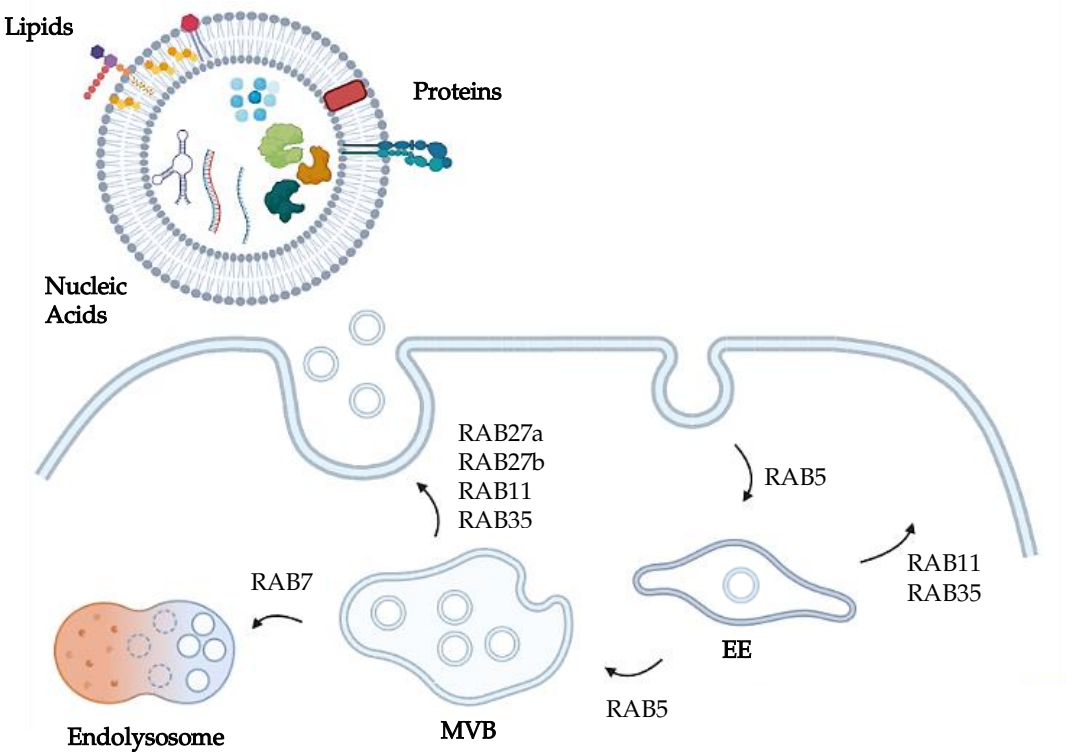

Figure 2. Schematic illustration of exosome biogenesis. EE – Early endosome; MVB – Multivesicular body. Created with BioRender.com.

1.7.2. Exosomes in the Pre-metastatic Niche Context

Exosomes are key mediators of tumour permissive niches, through induction of vascular leakiness, alteration of local resident cells, ECM remodelling, recruitment of non-resident cells such as bone marrow-derived cells (BMDCs), to name a few[152]. Disruption of vascular integrity is one of the earliest events implicated in the PMN establishment[152]. Zeng et al. reported that the exosomal transfer of the miR-25-3p from colorectal cancer cells to endothelial cells, provoked vascular leakiness and metastasis in liver and lung of mice[153]. miR-25-3p targets Krüppel-like factor (KLF) 2 and KLF4, which belong to a family of zinc finger-containing transcription factors[153]. KLF2 negatively regulates angiogenesis by reducing the promoter activity of VEGF receptor (VEGFR) 2, and KLF4 maintains integrity of endothelial barrier function by enhancing the promoter activity of tight junction related proteins including zonula occludens-1 (ZO-1), occludin, and claudin-5[153].

The PMN is also tightly related with recruitment of stromal residents[152]. Recent findings suggest that TGFβ-enriched exosomes released by bladder cancer cells are internalized by fibroblasts and trigger differentiation of these into CAFs[154]. Another study demonstrated that exosomes released by chronic lymphocytic leukaemia cells drive the adoption of an inflammatory phenotype similar to the phenotype of CAFs by endothelial and mesenchymal stem cells upon uptake[155]. The activated stromal cells showed enhanced proliferation, migration, and secretion of inflammatory cytokines, thus potentially leading to a permissive TME[155].

Moreover, changes in composition and organization of the ECM can foster PMN formation and metastatic colonization[156,157]. These changes can happen through altered deposition of ECM components and modification of physical properties of pre-existing ECM[152]. An example of increased deposition of an ECM component is the upregulation of fibronectin production by Kupffer cells in liver[158]. The uptake of pancreatic ductal adenocarcinoma-derived exosomes, containing macrophage migration inhibitor factor (MIF), by hepatic stellate cells in the liver caused TGFβ secretion, which in turn upregulated fibronectin production in Kupffer cells[158]. The deposition of fibronectin instigate a fibrotic environment favourable to metastatic growth through arrest of bone marrow-derived macrophages and neutrophils in the liver[158]. Furthermore, Hood et al. showed that injection of mouse B16-F10 melanoma exosomes increased gene expression of factors involved in cell recruitment, ECM modification, and vascular proliferation in sentinel node microenvironments promoting melanoma metastasis[157].

Finally, the mobilization of BMDCs contribute to PMN creation[152]. In fact, Kaplan et al. demonstrated that VEGFR1$^+$ hematopoietic progenitor cells formed cellular clusters before the arrival of tumour cells in pre-metastatic organs[159]. Removal of VEGFR1$^+$ cells from the bone marrow of wild-type mice or VEGFR1 antibody-mediated blockade impeded the formation of these pre-metastatic clusters, therefore preventing metastasis[159]. Notably, myeloid-derived suppressor cells (MDSCs), CD11b$^+$ Gr-1$^+$ tumour-infiltrating immature myeloid cells, are key mediators of the PMN formation and evolution[160]. Evidence points that cancer exosome-derived miR-9 and miR-181a contribute to expansion of early-stage MDSCs in breast cancer with high IL-6 expression, suppressing T-cell immunity and originating immunosuppressive niches.

1.7.3. Exosome Integrins and Organotropism

As Paget referred, "the distribution of secondary growths [metastases] is not a matter of chance"[129]. In a study comprising 2,147 patients with breast carcinoma, the incidence of lung metastases was 71%, bone 71%, lymph nodes 67%, liver 62%, pleura 50% and brain 22%[161]. By contrast, after autopsying 1,589 patients with prostate cancer, it was concluded that the most frequent metastatic sites were bone (90%), lung (46%), liver (25%), pleura (21%), and adrenals (13%)[162]. The reason why prostate cancer patients have increased probability of developing bone metastasis than breast cancer patients or why liver metastasis is more usual in prostate cancer than breast cancer patients can be explained by organotropic fusion of exosomes to promote PMN formation in specific organs[163]. Organ-specific metastasis is directed by the presence of integrins displayed on the surface of exosomes[164].

Integrins are a family of 24 transmembrane heterodimers that function as cell adhesion receptors for components of the ECM and are generated from a combination of 18 α and 8 β integrin subunits[165]. In order to exist, cells from multicellular organisms must be receptive to external input signals to live, proliferate, migrate and die in a controlled manner[166]. Integrins sense these inputs and mediate focal adhesion kinase (FAK) signalling pathway[166,167]. Integrins expressed in tumour cells contribute to tumour progression and metastasis by increasing tumour cell migration, invasion, proliferation and survival[168–170].

In 2015, Hoshino et al. demonstrated that exosomes isolated from lung-tropic 4175-LuT cell line (derived from a breast cancer adenocarcinoma cell line, MDA-MB-231, collected from the pleural effusion of a breast cancer patient) were enriched in integrins $\alpha_6\beta_1$ and $\alpha_6\beta_4$[164]. These exosomes mainly co-localized with S100A4+ fibroblasts and surfactant protein C (SPC)+ epithelial cells in laminin-rich lung microenvironments, when intravenously injected in mice[164]. Since these receptors bind laminin, these exosomal integrins may selectively fuse with resident cells in these areas[171]. The exosomal uptake induced Src activation and upregulation of pro-migratory and pro-inflammatory S100 molecules on resident cells, educating these cells to prepare the PMN[164]. Targeting integrins $\alpha_6\beta_1$ and $\alpha_6\beta_4$ decreased exosome uptake and impaired lung metastasis[164]. While exosomal integrins $\alpha_6\beta_1$ and $\alpha_6\beta_4$ were connected to lung metastasis, exosomal integrin $\alpha_v\beta_5$ was linked to liver metastasis by arresting in fibronectin-rich liver microenvironments and fusion with Kupffer cells[164]. Furthermore, exosomal integrins $\alpha_v\beta_6$, $\alpha_v\beta_3$ and $\alpha_4\beta_1$ were associated to bone metastases and exosomal integrins $\alpha_4\beta_1$ and $\alpha_4\beta_7$ to lymph nodes metastases[163,172–174].

1.8. Blocking the Invasion and Metastasis Hallmark

At the current time, a diagnosis of metastatic disease is synonym of terminal illness for the great majority of cases[175]. From 2005 to 2015, few improvements were verified in the 5-year survival of cancer patients initially diagnosed with metastatic disease, with only 1 of the 12 types of cancer assessed showing a survival gain of more than 3%[175]. These facts can be explained by the lack of effective therapies[176]. Excluding surgery, the current therapeutics strategies for eliminating metastases are essentially the same as those used to target primary tumors[176]. Given that metastatic lesions derive from a subclonal minority within the primary tumour and that this subpopulation can be further subjected to evolutionary pressures at the second site, the level of genetic and epigenetic heterogeneity between neoplastic cells at the primary and secondary sites may be presumably high[44,177–180]. From this perspective, it seems logical that cancer therapies that aim to interfere with a single pathway and provoke an effective response in patients with localized disease may not reveal an anti-metastatic effect[178]. The targeting of the multistage process of metastasis can be achieved by interfering with steps of the invasion-metastasis cascade[95]. Despite existing a long list of metastasis-directed drugs that passed preclinical validation, few exhibited a positive outcome in clinical trials[175,181,182]. Denosumab, a humanized monoclonal antibody, is a fortunate example of a drug approved by the United States Food and Drug Administration (FDA) and the European Medicines Agency (EMA), indicated to treat bone metastasis[183–187]. To understand its mechanism of action, it is important to be aware that, at the arrival, DTCs activate osteoblasts to secrete receptor activator of NF-κB ligand (RANKL)[183]. In turn, RANKL activates osteoclasts to

degrade bone and, by doing so, factors, such as TGFβ, are released from the bone matrix activating tumour cells and reinitiating the cycle[183]. The anti-metastatic agent Denosumab inhibits RANKL, interrupting this "vicious cycle" and preventing osteolytic lesions[183]. Denosumab uncover the clinical value of disrupting heterotypical interactions within the TME.

The capability of invading into the surrounding tissues and metastasizing at distant organs is the most defining feature of malignancy[188]. Hence, it is urgent to develop new effective therapies that halt this hallmark. At the light of this thinking, antisense oligonucleotides (ASOs) have been developed as an innovative strategy to stop cancer.

1.9. Antisense Oligonucleotides Therapeutics

Classical anticancer drugs comprise small molecules (possessing <100 atoms) with hydrophobic character, permitting rapid passive diffusion across plasma membranes, and target proteins with hydrophobic pockets[189]. Other conventional protein-based drug modalities, with higher molecular weight, are essentially restricted to extracellular targets because they are unable to traverse the cellular barrier[189]. Some key oncogenic driver proteins, such as MYC and KRAS, were therefore termed "undruggable" owing to their intracellular location, their large protein–protein interaction interfaces or their lack of deep protein pockets[190]. Targeting the carriers of genetic information before being translated into proteins, in the other side of the coin, allows a broader therapeutic spectrum[191].

The number of nucleic acid-based therapeutics approved by EMA and FDA have been escalating in the last few years[192]. On top of that, they were placed under the spotlight with the worldwide administration of the two COVID-19 mRNA-based vaccines, Moderna's mRNA-1273 and Pfizer/BioNTech's BNT162b2[193,194]. Nucleic acid therapeutics modulate gene expression by inhibiting, adding, replacing or editing at the DNA or RNA levels[192]. If the mechanism of action occurs at the RNA level, they fall into the category of RNA-targeted therapeutics that include ASOs, small interfering RNAs (siRNAs), aptamers, microRNAs (miRNAs), and messenger RNAs (mRNAs)[195].

ASOs, in particular, are single-stranded DNA molecules ranging in size from 18 to 30 bps[196,197]. They act by redirecting alternative splicing, blocking the access of translational machinery to mRNA and/or recruiting ribonuclease H1 (RNase H1) leading to target degradation[197–201]. RNase H1 is an ubiquitous cellular enzyme that recognizes DNA-RNA hybrids and cleaves the RNA molecule in the hybrid[197]. ASOs are the leading bet on oligonucleotide therapeutics, with the highest number of clinical trials based on this technology at the moment and at least 10 ASO drugs approved by regulatory entities[202,203]. Inotersen, sold under the name of Tegsedi, is an example of one of these[204]. It is an antisense drug that prevents production of the transthyretin protein by an RNase H1 dependent mechanism indicated to treat hereditary amyloidogenic transthyretin (ATTRv) amyloidosis[203,205,206]. ATTRv amyloidosis was first described as familial amyloid polyneuropathy (FAP) in northern Portugal, an endemic region to this disease[205]. The condition provokes extracellular deposition of amyloid and progressive destruction of the somatic and autonomic peripheral nervous system (PNS) that leads to loss of autonomy and

death[205]. Inotersen reduces the production of transthyretin, halting the progression of the disease and preventing aggravation of the symptoms.

Oligonucleotides are typically large, hydrophilic polyanions, which impedes them of easily cross the plasma membrane[203,207,208]. Furthermore, systemically injected nucleic acid drugs are subjected to nuclease degradation, renal clearance, removal by the reticuloendothelial system, once inside the cell, lysosomal degradation or re-export via exocytosis, and may even induce an undesired immune response[203,209–214]. Systemic delivery to the central nervous system (CNS) has the additional complication of passing through blood-brain barrier (BBB)[203]. To circumvent these drawbacks, oligonucleotides can be chemically modified, conjugated with biomolecules, and attached to/encapsulated inside nanoparticles[209,215,216]. Attending to the astonishing, wide range of medical diagnostic and therapeutic applications of gold nanoparticles (AuNPs), some predict a new "Golden Age" for biomedical nanotechnology[217]. In sequence, AuNPs are extremely useful in the delivery of ASOs[218].

1.9.1. Gold Nanoparticles for Antisense Oligonucleotides Delivery

Nanomedicine is a cross-disciplinary area originated from the application of nanotechnology to medicine[219]. The design and use of nanomaterials to drug delivery, vaccine development, diagnosis and imaging tools, high-throughput screening platforms, among others, have been gaining much attention[220]. In opposition to atoms and macroscopic materials, nanomaterials have a high ratio of surface area to volume, tuneable optical, electronic, magnetic, and biologic properties, and they can be manipulated to have different sizes, shapes, chemical compositions, surface chemical characteristics, and structures[221]. Concretely, AuNPs are of great interest in cancer nanomedicine[217,222].

Colloidal AuNPs have been used since ancient times to stain glass due to their optical properties[223,224]. The distinct optical properties of these small metal nanoparticles are given by collective oscillations of electrons in resonance with the incident electromagnetic radiation, phenomenon termed localized surface plasmon resonance (LSPR)[223,225,226]. In cancer nanomedicine, AuNPs generally have dimensions included in the 5-100 nm size range and hold great potential as drug delivery agents, enhancers in plasmonic photothermal therapy, and in sensing/diagnostics applications[227–231]. This type of nanomaterials is considered to be inert and nontoxic at estimated therapeutic concentrations (except for some modified cationic AuNPs)[226,232–237]. AuNPs can be further functionalized with capping agents, such as polyethylene glycol (PEG), to improve their *in vivo* stability and to avoid uptake by the reticular endothelial system[238–243]. Key properties, such as biocompatibility, tuneable size, and straightforward functionalization, make them attractive scaffolds for the creation of nucleic acid delivery vehicles[244,245].

When loaded on AuNPs, ASOs are less susceptible to degradation by nuclease activity, cellular uptake increases significatively and oligonucleotides enter the intracellular space at a higher effective concentration than conventional transfection agents due to the large surface area of nanoparticles[245–247]. These nanocarriers can take advantage of leaky vasculature and defective lymphatic drainage of tumours [enhanced permeability and retention (EPR) effect] to cross endothelial barriers thereby benefiting from passive targeting[248–250]. On the other

hand, nanoformulations can also include targeting ligands and pH-activated proteins that enhance cellular internalization by target cells and aid in the endosomal escape, respectively[249,251]. Some articles were already published reporting successful gene silencing using PEGylated AuNPs as delivery vehicles for nucleic acids *in vitro*, demonstrating the enormous therapeutic potential of these nanostrategies[252–256]. Moreover, expectations keep climbing, especially after the release of results concerning the first-in-human phase 0 clinical trial (NCT03020017) to study the safety, pharmacokinetics, intratumoral accumulation and gene-suppressive activity of AuNPs covalently conjugated with siRNAs[257]. The drug was designed to target Bcl-2-like protein 12 (BCL2L12) transcripts on recurrent glioblastoma multiforme or gliosarcoma patients[257]. Results were encouraging: no significant treatment-related toxicities were determined by safety assessment; low levels of AuNPs were detected in plasma of treated patients; AuNPs enrichment was observed in tumour-associated endothelium, macrophages and tumour cells; and significant reduction in tumour-associated Bcl2L12 protein expression was noted[257]. This landmark study is another step forward towards the "Golden Age".

1.10. Scope of the Thesis

The major objective of this work is to inhibit the breast cancer cells-derived exosomes uptake by lung cells to avoid PMN formation. This thesis constitutes a first endeavour to silence *ITGA6* expression with the view to inhibit the synthesis of this protein subunit and the assembly of integrins $\alpha_6\beta_1$ and $\alpha_6\beta_4$. To achieve the stated purpose, an antisense sequence that selectively targets *ITGA6* transcripts was identified. A hybridization analysis *in silico* was made to assess the gene silencing potential of the designed oligonucleotide. AuNPs were PEGylated, functionalized with the ASO and characterized. Breast adenocarcinoma MDA-MB-231 cell line was carefully selected to test the silencing efficacy of Au-nanoconjugates *in vitro*. This cell line metastasizes primarily to the lung and releases lung tropic exosomes enriched in integrins $\alpha_6\beta_1$ and $\alpha_6\beta_4$. The depletion of integrins $\alpha_6\beta_1$ and $\alpha_6\beta_4$ levels have great therapeutic potential since reducing the availability of these surface receptors for packaging into exosomes disrupts integrin-mediated lung tropic metastasis. The *ITGA6* knockdown was verified at the RNA level, through RT-qPCR, and at the protein expression level, through western blot. Additionally, an attachment assay was executed to evaluate differences in cell adhesion capability between treated and untreated cells.

| 2.

MATERIALS AND METHODS

2.1. Materials

2.1.1. Reagents

- 25 cm^2 culture flasks (SPL)
- Acetic acid (Merck, CAS no. 64-19-7 | 100063)
- Acrylamide-bisacrylamide (37.5:1) (Merck, Cat. no. 100638)
- Agarose (NZYtech, CAS no. 9012-36-6)
- Amersham Protran 0.45 µm nitrocellulose membrane (GE Healthcare)
- Anti-integrin alpha 6 antibody [EPR18124] (Abcam, Cat. no. ab181551)
- Anti-integrin beta 4 antibody [M126] (Abcam, Cat. no. ab29042)
- Anti-mouse IgG, HRP-linked Antibody (Cell Signaling Technology, Cat. no. 7076)
- Anti-rabbit IgG, HRP-linked Antibody (Cell Signaling Technology, Cat. no. 7074)]
- Anti-β-actin antibody (Sigma-Aldrich, Cat. no. A5441)
- Bromophenol blue (Merck, CAS no. 115-39-9)
- Diethyl pyrocarbonate (DEPC; Sigma-Aldrich, CAS no.1609-47-8)
- Disodium phosphate (Sigma-Aldrich, CAS no. 7558-79-4)
- Dithiothreitol (DTT; Sigma-Aldrich, CAS no. 3483-12-3)
- Dulbecco's modified eagle medium (DMEM; Gibco, ThermoFisher Scientific)
- EASYpack Protease Inhibitor Cocktail (Roche, Cat. no. 05 892 791 001)
- Ethyl acetate (Merck, CAS no. 141-78-6)
- Ethylenediamine tetraacetic acid, EDTA diNa salt.2aq (CAS: 6381-92-6)
- Foetal bovine Serum (FBS; Gibco, ThermoFisher Scientific)
- GAPDH primers (STABVIDA)
- GelRed (Biotium, Cat. no. 41003)
- GeneRuler DNA Ladder Mix (ThermoFisher Scientific, Cat. no. SM0331)
- Glycerol (Amresco, CAS no. 56-81-5)
- Glycine (Sigma-Aldrich, CAS no. 56-40-6)
- Hyperfilm ECL (GE Healthcare)
- Illustra NAP-5 column (GE Healthcare Life Sciences, Cat. no. 17-0853-02)

- ITGA6 primers (STABVIDA)
- Magnesium acetate (Sigma-Aldrich, CAS no. 16674-78-5)
- MDA-MB-231 (ATCC HTB-26)
- MEM nonessential amino acid (Gibco, ThermoFisher Scientific)
- Mini-Sub Cell GT Cell (Bio-Rad)
- NP-40 (Surfact-Amps, ThermoFisher Scientific)
- O-(2-Mercaptoethyl)-O′-methyl-hexa(ethylene glycol) (*m*PEG thiol; Sigma-Aldrich, CAS no. 651042-82-9)
- One-step NZY RT-qPCR Green kit (NZYtech, Cat no. MB343)
- Penicillin-streptomycin (Gibco, ThermoFisher Scientific; Cat. no. 15140122)
- Phenylmethylsulfonyl fluoride (PMSF; Sigma-Aldrich, CAS no. 329-98-6)
- PhosStop Phosphatase Inhibitor Cocktail (Roche, Cat. no. 04 906 845 001)
- Pierce 660nm Protein Assay Reagent (ThermoFisher Scientific, Cat. no. 1861426)
- Pierce Bovine Serum Albumin Standard Pre-Diluted Set (ThermoFisher Scientific, Cat. no. 23208)
- Polystyrene cuvettes (Sarstedt, Cat. no. 67.742)
- Potassium chloride (Merck, CAS no. 7447-40-7)
- PowerPac Basic Power Supply (Bio-Rad)
- Skimmed milk 0% fat (Régilait)
- Sodium chloride (NaCl; Sigma-Aldrich, CAS no. 7647-14-5)
- Sodium dodecyl sulphate (SDS; Merck, CAS no. 151-21-3)
- Sodium hydroxide (NaOH; Sigma-Aldrich, CAS no. 1310-73-2)
- Sodium phosphate, monohydrated (Merck, CAS no. 10049-21-5)
- Tris buffer (Fisher Bioreagents, CAS no. 77-86-1)
- Trypan blue solution (ThermoFisher Scientific, Cat. no. 15250061)
- TrypLE Express (Gibco, ThermoFisher Scientific)
- Tween 20 (Sigma-Aldrich, CAS: 9005-64-5)
- WesternBright ECL (Advansta)

2.1.2. Equipment

- 5424 R centrifuge (Eppendorf)
- CXX41 inverted microscope (Olympus)
- Elmasonic S10 H ultrasonic bath (Elma)
- Gel DocTM EZ Imager (Bio-Rad)
- Microplate reader Infinite F200 (Tecan)
- Nanodrop ND-1000 spectrophotometer (Thermo Fischer Scientific)
- Rotor-Gene Q (Qiagen)
- Sanyo CO_2 Incubator (Electric Biomedical Co.)
- Sigma 1-14K centrifuge (Sigma-Aldrich)
- Ti-U Eclipse inverted microscope (Nikon)
- UVmini-1240 spectrophotometer (Shimadzu)

- Zetasizer NanoZS ZEN 3500 (Malvern)

2.2. Methods

2.2.1. Hairpin Design and Hybridization Analysis *in Silico*

The choice of the oligonucleotide sequence and the modifications effected are detailed in section 3.1. For the hybridization analysis, it was used the NUPACK Web Application (http://www.nupack.org/)[258] with default settings. The RNAfold web server (http://rna.tbi.univie.ac.at/cgi-bin/RNAWebSuite/RNAfold.cgi)[259] created by the University of Vienna was employed in the self-hybridization analysis, considering the entire *ITGA6* mRNA sequence. This analysis was carried out to forecast the possibility of the ASO biding region being occupied, due to hydrogen bonds with distant regions of the molecule. A BLAST (Basic Local Alignment Search Tool; https://blast.ncbi.nlm.nih.gov/Blast .cgi?PROGRAM=blastn&PAGE_TYPE=BlastSearch&LINK_LOC=blasthome) search was made choosing the *Human G+T* database and selecting the *blastn* program. Also, some algorithm parameters were changed to accomplish a broader range of results (*Expected threshold* = 100; *Word size* = 7; *Match/Mismatch Scores* = 1,-3; *Gap Costs* = Existence: 0 Extension: 2; *Filters and Masking* = None). For all analysis involving *ITGA6* mRNA sequence, ITGA6 cDNA sequence available on the Ensembl website was utilized – Ensemble ID: ENST00000264107.12.

2.2.2. Functionalization of Gold Nanoparticles

AuNPs, with approximately 14 nm, were synthesized by Dr. Luís Raposo using the citrate-reduction method[260,261] (AuNPs@citrate) and were ceded for the present experimental work. The colloidal stability was confirmed by comparing the wavelength corresponding to the localized surface plasmon resonance (LSPR) band on the absorption spectra taken at the time of synthesis and at each round of functionalization. All absorbance measurements involving nanoparticles were made using the UVmini-1240 spectrophotometer and polystyrene cuvettes. Before each measurement, the colloidal solution was sonicated for about 2 min with the purpose of dispersing the AuNPs and ensuring that there was no variation of concentrations within the same volume. Whenever possible, the solvents and buffers in which AuNPs were dissolved, were sterilized by filtration (0.22 μm) and autoclaved. All reagents utilized were dissolved in ultrapure water (18.2 MΩ × cm at 25 °C) except when specified otherwise.

2.2.2.1. PEGylation of Gold Nanoparticles

The concentration of AuNPs in solution was determined resorting to the Lambert-Beer law ($A = \varepsilon \times l \times c$, where A is the absorbance, ε is the molar absorptivity, l is the optical path length and c the concentration), assuming a molar extinction coefficient of 2.33×10^{-8} $M^{-1}cm^{-1}$ [262]. Thereafter, it was prepared a reactional mixture with a final volume of 10 mL containing 10 nM AuNPs, 0.028% (w/v) SDS and 0.003 mg/mL *m*PEG thiol. This protocol had previously been optimized in the lab[262]. The mixture was incubated over 10 min at room temperature while stirring. Having finished that period of time, it was added 125 μL of 2 M NaOH and the

mixture was left overnight under the same conditions as before. The next day, the volume of PEGylated AuNPs was distributed into six centrifuge tubes of 2 mL and centrifuged for 20 min at 21,000 × g employing the 5424 R centrifuge. In order to remove PEG in excess, the precipitate was then washed one time with ultrapure water and another time with DEPC - treated water [0.1% (v/v)]. PEGylated AuNPs (AuNPs@PEG) were stored at 4 °C in a volume of around 1 mL.

2.2.2.2. Functionalization of PEGylated Gold Nanoparticles with Antisense Hairpin DNA

AuNPs@PEG were further functionalized with an antisense ITGA6 oligonucleotide in hairpin conformation. The thiolated oligonucleotide was resuspended in 1 mL of 0.1 M DTT for 2 hours at 4 °C, in order to reduce disulphide bonds. The sample was then washed with two volumes of ethyl acetate for three times. The steps of centrifugation between washes were done with a duration of 5 min at 21,000 × g using the 5424 R centrifuge. The remaining aqueous phase was purified using a desalting Illustra NAP-5 column and 10 mM phosphate buffer pH 8 (9.32 mM disodium phosphate; 0.68 mM sodium phosphate, monohydrated) as eluent.

The hairpin concentration was calculated resorting to the absorbance given by the Nanodrop and the extinction coefficient at 260 nm described on the product specifications provided by the manufacturer. The volume of purified oligonucleotide needed to attain a ratio of 152:1 (AuNP:oligonucleotide) was mixed with the volume of AuNPs@PEG that could be dispensed. Subsequently, it was added AGE I solution – 2% (w/v) SDS in 10 mM phosphate buffer pH 8 – to a final concentration of 0.01% SDS (w/v). The mixture was incubated for 20 min at room temperature. Volumes of AGE II solution – 1.5 M NaCl in AGE I solution – required for the final concentrations 0.05, 0.1, 0.2 and 0.3 M of NaCl were sequentially pipetted to the reactional mixture. After each addition, the mixture was submitted to sonication for 1 min in the ultrasonic bath and incubated for 20 minutes at room temperature. Following the last addition, the mixture was incubated for 16 hours at room temperature in the dark. The next day, the solution containing AuNPs functionalized with PEG and antisense-ITGA6 (AunNPs@PEG@ITGA6) was centrifuged using the same equipment as earlier for 20 min at 21,000 × g to remove the oligonucleotide that did not bound. The quantity of oligonucleotide molecules that stayed in the supernatant were quantified employing the Nanodrop. The binding efficiency was determined subtracting the remaining oligo quantity to the initially applied quantity. The precipitate was redispersed in 1 mL of DEPC-treated water.

2.2.2.3. Characterization of Functionalized Gold Nanoparticles

The AuNPs were characterized by ultraviolet-visible (UV-Vis) spectroscopy using the UVmini-1240 spectrophotometer and the hydrodynamic particle diameter was ascertained by dynamic light scattering (DLS) using the Zetasizer NanoZS ZEN 3500. The AuNP formulations were diluted in ultrapure water to a final concentration of 2 nM and sonicated prior to analysis.

2.2.3. Cell Culture

The breast adenocarcinoma cell line MDA-MB-231 (ATCC HTB-26) used for the silencing experiment was grown in DMEM and supplemented with 10% (v/v) FBS, a mixture of 100 U/mL penicillin and 100 µg/mL streptomycin, and 1% (v/v) MEM nonessential amino acid. Cells were maintained in 25 cm^2 culture flasks (SPL) at 37 ºC in a 99% (v/v) humidified atmosphere of 5% (v/v) CO_2. These are the CO_2 incubator conditions used throughout all the procedures. Analysis of mycoplasma was performed every 15 days in the laboratory, through PCR testing.

Culture cells were passaged when an 80% confluence was reached. After the medium was removed and discarded, 2 mL of TrypLE Express were added to the flask so adherent cells could detach. After the time needed for that purpose, 1 mL of medium was added to stop the enzymatic activity. The cell suspension was transferred to centrifugation tubes and centrifuged for 5 min, 500 × g, room temperature in the Sigma 1-14K centrifuge. Afterwards, the supernatant was discarded, and the remaining pellet was resuspended in 1 mL of fresh medium. Cell density was verified using a 0.4% trypan blue solution to assess viable cells, on the inverted microscope Olympus CXX41. The volume of cellular suspension needed to obtain a cell density of 2.5×10^4 cells/mL was transferred to a new flask with 5 mL of medium, being afterwards incubated in the previously described conditions.

2.2.4. Gene Expression Analysis

For each condition/replicate, 500 µL of cell suspension at 1.5×10^5 cells/mL were plated into a 24-well plate and were left to adhere for 24 h in the CO_2 incubator. The next day, the medium was replaced by medium without (CTRL) or with 0.19 nM nanoconjugate (AuNPs@PEG or AuNPs@PEG@ITGA6). The exposure times 6, 14, 24, 48 and 72 h were tested. Passed the exposure time, the RNA extraction was performed following the NZYol protocol (NZYtech, Cat. no. MB18501). The RNA concentration was determined using the Nanodrop. The RNA integrity was assessed by the 260/280 and 260/230 absorbance ratios and by running a total RNA 0.8% agarose gel electrophoresis in TAE (tris-acetate-EDTA; 40mM Tris base, 20 mM acetic acid e 1mM EDTA) buffer with 2% (v/v) of GelRed, during 50 min at 90 V (horizontal electrophoresis system – Mini-Sub Cell GT Cell; electrophoresis power supply – PowerPac Basic Power Supply; gel imaging system- Gel DocTM EZ Imager). Samples were stored at -80 °C until further use.

The *ITGA6* silencing efficacy was evaluated by quantitative reverse transcription PCR (RT-qPCR) resorting to Rotor-Gene Q and using the One-step NZY RT-qPCR Green kit. The reaction conditions are described in Table 1. ITGA6 primer sequences[263]: forward – 5′-GAG CTT TTG TGA TGG GCG ATT-3′; reverse – 5′-CTC TCC ACC AAC TTC ATA AGG C-3′. Regarding the house keeping gene, the selected one was *GAPDH* since the primers were available in the lab and have been already tested and used. GAPDH primer sequences: forward – 5′-GAA GGT GAA GGT CGG AGT C-3′; reverse – 5′-GAA GAT GGT GAT GGG ATT TC-3′. The *ITGA6* gene expression was analysed by relative quantification, calculated by the $2^{-\Delta\Delta Ct}$ method[264]. All amplification products were then separated by gel electrophoresis, in a 2% (w/v) agarose gel using the same reagents and equipment reported for the total RNA electrophoresis. GeneRuler DNA Ladder Mix was used as molecular weight marker.

Table 1. RT-qPCR cycling conditions.

Cycles	Temperature	Time	Main reaction
1	50 °C	20 min	Reverse transcription
1	95 °C	10 min	Polymerase activation
35	95 °C	30 s	Denaturation
	60 °C	30 s	Annealing
	72 °C	40 s	Extension

2.2.5. Western Blot

For the relative protein quantification, cell seeding was carried out by transferring 2 mL of cell suspension at 1.5 × 10^5 cells/mL to a 6-well plate per condition/replicate. The culture plates were incubated for 24 h to allow cell attachment in the CO_2 incubator. The medium was changed by fresh medium with 0.19 nM Au-nanoconjugates and cells were incubated for 48 h. Having finished that period of time, cells were washed two times with phosphate buffered saline buffer 1× (PBS; 137 mM sodium chloride, 2.7 mM potassium chloride, 8 mM sodium phosphate, 2 mM disodium phosphate, pH 7.4) and scrapped using a cell scraper. The biological samples were then centrifuged for 5 min at 750 × g and 4 °C. To the pellet of cells was added a NP-40 cell lysis buffer [150 mM sodium chloride, 50 mM tris buffer (pH 8.0), 5 mM EDTA, 2% (v/v) NP-40, 1× PhosStop Phosphatase Inhibitor Cocktail, 1× EASYpack Protease Inhibitor Cocktail, 1 mM PMSF, and 0.1 % (w/v) DTT]. Whole-cell extracts were sonicated, with six cycles of 3 min (2 min 30 s of sonication and 30 s of pause), and subsequently centrifuged at 5000 × g for 10 min at 4 °C. The supernatant was recovered, and protein concentration was determined using the Pierce 660nm Protein Assay Reagent according to the manufacturer's specifications. A calibration curve was made employing the Pierce Bovine Serum Albumin Standard Pre-Diluted Set. The 660 nm absorbance was acquired on the microplates reader Infinite F200. After that, 25 µg total protein extracts were treated with SDS loading buffer (1×) [SDS loading buffer 5×: 0.25% (w/v) bromophenol blue; 500 mM DTT; 20% (v/v) glycerol; 10% (w/v) SDS; 250 mM tris buffer (pH 6.8)], heated at 90 °C for 5 min, and incubated for 2 h at room temperature. Samples were separated by SDS-PAGE (SDS-polyacrylamide gel electrophoresis) in an 8% (w/v) (37.5:1) acrylamide-bisacrylamide gel.

Afterwards, it was executed a semi-dry electrophoretic transfer onto an Amersham Protran 0.45 µm nitrocellulose membrane. The blocking was performed with a 5 % (w/v) milk solution in tris-buffered saline with 0.1 % (v/v) tween 20 (TBST; 50 mM tris, 150 mM NaCl e 0,1% (v/v) tween 20, pH= 7,5). Blots were incubated, according to the manufacturer's instructions, with primary antibodies anti-integrin beta 4 antibody [M126] (dil. 1:1000), anti-integrin alpha 6 antibody [EPR18124] (dil. 1:2000) and anti-β-actin antibody (dil. 1:5000). Membranes were washed three times with TBST during periods of 5 min and incubated with the appropriate secondary antibody conjugated with horseradish peroxidase [anti-mouse IgG, HRP-linked Antibody (1:3000) or anti-rabbit IgG, HRP-linked Antibody (1:2000)]. Again, membranes were washed three times with TBST during periods of 5 min. WesternBright ECL (Advansta) was applied to the membranes, and signal was acquired on an X-ray film, Hyperfilm ECL. Band quantification was made using the ImageJ software

(https://imagej.nih.gov/ij/)[265] selecting the adequate blot band in a rectangle with the same area. Membranes were treated with a stripping solution (0.1 M glycine, 20 mM magnesium acetate, 50 mM potassium chloride, pH 2) between incubations with different primary antibodies.

2.2.6. Attachment Assay

To understand if the ITGA6 silencing produced a phenotypical change, an assay was conducted in which seeding was made at 1.5×10^5 cells/mL and at 1.0×10^4 cells/mL in 6-well plates. The cell cultures were incubated for 24 h in the CO_2 Incubator to allow cell adhesion. After that, cells were exposed to medium, 0.19 nM AuNP@PEG and 0.19 nM AuNP@PEG@ITGA6 for 48 h in the same incubator. Having finished that period of time, cells were incubated with 2 mL of TrypLE Express, so cells could detach. TrypLE Express was inhibited by adding medium, and cells were centrifuged for 5 min at 500 × g in Sigma 1-14K centrifuge. Cells were then transferred once more to 6-well plates at the same cell density and incubated for 5 h in the incubator mentioned previously. Afterwards, the medium was aspirated and was added 1 mL of fresh medium. The cells were then counted by capturing 5 images of different well regions using a low magnification objective (10×) of Ti-U Eclipse inverted microscope (Nikon). The average number of cells counted in 5 images/well were converted in cells/cm^2.

| 3.

RESULTS AND DISCUSSION

3.1. Hairpin Design and Hybridization Analysis *in Silico*

In order to silence the gene of interest, *ITGA6*, an antisense hairpin oligonucleotide was designed – 5-Thiol-C6-TTTCGGTTAACCTGGAGGCATATCCCCGAAA-3' (palindromic sequence underlined). The *ITGA6* mRNA antisense sequence was selected from the literature[266–268], and had previously shown to effectively silence this gene. The ASO was modified with 5'–thiol-C6 and was flanked by two palindromic regions, described in[252], to induce a hairpin conformation. The hairpin conformation increases the oligonucleotide selectivity, by ensuring the hairpin will only open in the presence of a fully complementary target[269]. Its ability to interrupt ITGA6 synthesis was evaluated *in silico* by a) determining the hairpin secondary structure corresponding to the MFE structure (Figure 3) b) confirming a decrease in free energy caused by the hairpin-target bond (Figure 4) c) checking if the binding segment in the *ITGA6* transcript has low self-hybridization probability (Figure 5) and d) assessing the hairpin specificity through the BLAST bioinformatic tool.

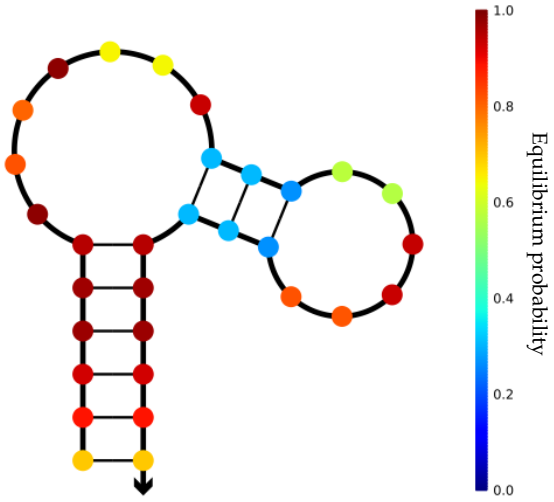

Figure 3. MFE structure of the designed antisense hairpin. This image was obtained from the NUPACK Web Application[258]. The predicted MFE secondary structure was calculated submitting the developed hairpin sequence with the default NUPACK settings.

Focusing on Figure 3, it is noticeable a secondary structure with two stem-loops, one associated to a high probability pairing region (≈1.0) with an extent of six bps, and another associated to a low probability pairing region (≈0.3) with only three bps. The most stable and longest stem-loop was formed by the addition of the flanking palindromic sequence to the

ITGA6 mRNAs complementary sequence and seems to successfully induce a hairpin conformation. The most unsteady and shortest secondary structure does not appear to constitute an obstacle to the hairpin-target interaction, once it presents weak probability of forming hydrogen bonds at 37 °C. Even so, free energy values of the MFE structure of a fragment of 419 nucleotides with and without the binding of the hairpin were determined resorting to the NUPACK program, Figure 4. Thereby, it was possible to understand if the hybridization between the antisense oligonucleotide and the mRNA target is thermodynamically favoured. Without interacting with the antisense hairpin, the transcript MFE structure has a free energy of -83.40 kcal/mol. On the other hand, once the hairpin is paired with the transcript, the free energy of the system drops to -106.78 kcal/mol. Thus, it is viable to say that there is a tendency towards the generation of the hairpin-target complex.

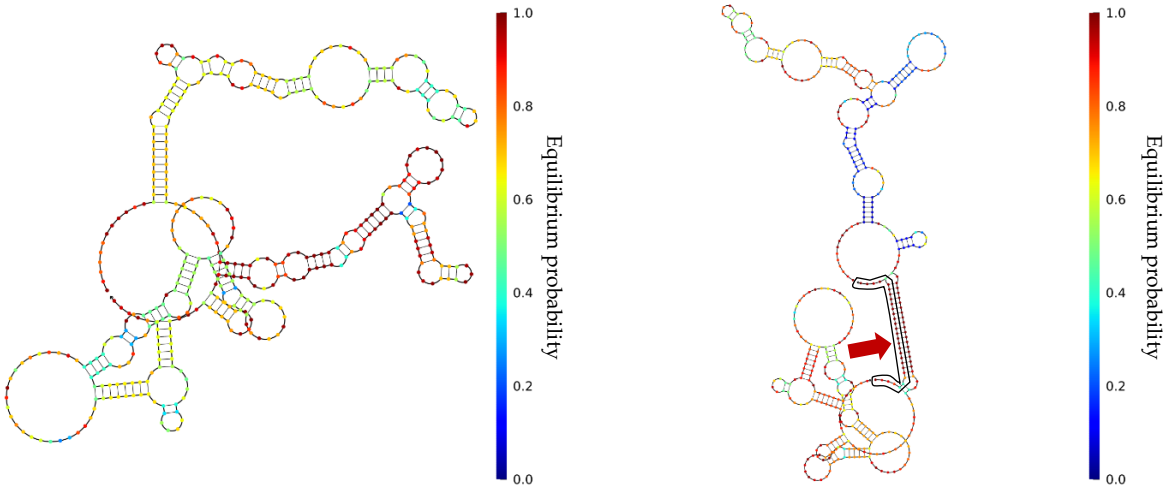

Free energy of secondary structure: -83.40 kcal/mol

Free energy of secondary structure: -106.78 kcal/mol

Figure 4. Impact of the antisense hairpin hybridization on the MFE structure of a fragment of the *ITGA6* transcript. A segment of 419 nucleotides (nucleotides 1515-1933 from the ITGA6 cDNA sequence available on the Ensembl website – Ensemble ID: ENST00000264107.12) containing the hairpin complementary sequence, figure on the **left**, and this same segment submitted along with the designed hairpin, figure on the **right**, were analysed using the NUPACK Web Application[258] with the default settings. Under each structure is stated the respective free energy value. The hairpin is surrounded in black and marked with a red arrow.

Furthermore, and since the NUPACK program does not accept sequences with size equivalent to the whole *ITGA6* mRNA (>5600 nucleotides), it was made a new analysis using the RNAfold web server. By doing so, it was ascertained the probability of hybridization between the hairpin complementary region and other distant segments of the *ITGA6* transcript. The Figure 5 shows that self-hybridization probability on the hairpin binding site is very reduced.

With regard to the BLAST analysis, the results revealed that the hairpin had affinity to all *ITGA6* transcript variants, establishing hydrogen bonds with a continuous sequence of 20 nucleotides. Alongside, the hairpin had propensity to interact with 15 consecutive nucleotides of two transcript variants of a long non-coding RNA, Long Intergenic Non-protein Coding RNA 1255 (LINC01255). In any case, the *ITGA6* transcript has a longer complementary sequence.

Together, these findings suggest that the designed antisense short hairpin DNA has the potential to induce *ITGA6* silencing.

Figure 5. Self-hybridization probability of *ITGA6* transcript. The mRNA sequence is coloured according to the probability of self-hybridization. The ASO binding region is zoomed in on the oval window where is possible to discriminate the complementary sequence (inside the rectangle with black contours). This image was obtained from the RNAfold web server created by the University of Vienna[259]. The predicted MFE secondary structure was calculated submitting the ITGA6 cDNA sequence (available on the Ensembl website; Ensemble ID: ENST00000264107.12) with the default settings.

3.2. Functionalization and Characterization of AuNPs

Once the hairpin was designed, AuNPs previously synthetized by Dr. Luís Raposo were functionalized primarily with PEG and afterwards with the antisense hairpin. PEG chains play a decisive role on the protection of nanoparticles surface from aggregation, opsonization, and phagocytosis, hence improving the nanostructure stability and prolonging systemic circulation time[239,254,270]. To enable the binding of subsequent thiolated components, AuNPs were functionalized with the quantity of PEG molecules needed to attain a surface coverage of approximately 30%[253,271]. This proportion of spacer/DNA is sufficient for reaching the benefits described[272]. The NP:ASO ratio calculated by subtracting the oligo that remained in the supernatant after the functionalization was 1:104, a ratio commonly obtained using this AuNPs functionalization conditions[255].

To confirm if each functionalization step was achieved, AuNPs were characterized by UV-Vis spectroscopy and DLS. As visible in the first derivative spectra (Figure 6), after PEGylation, the LSPR band in the UV-Vis spectrum shifted by 1 nm to longer wavelengths and shifted an additional 3 nm from the PEGylated to the DNA-loaded AuNPs. This red shift is attributed to the alteration of the dielectric constant in the AuNPs surroundings[273–276]. Therefore, the information taken by the analysis of the spectra supports that the functionalization occurred. The hydrodynamic diameter distribution curves (Figure 7) show AuNPs@citrate have an average diameter of 12.67 ± 3.21 nm, AuNPs@PEG of 34.22 ± 4.23 nm

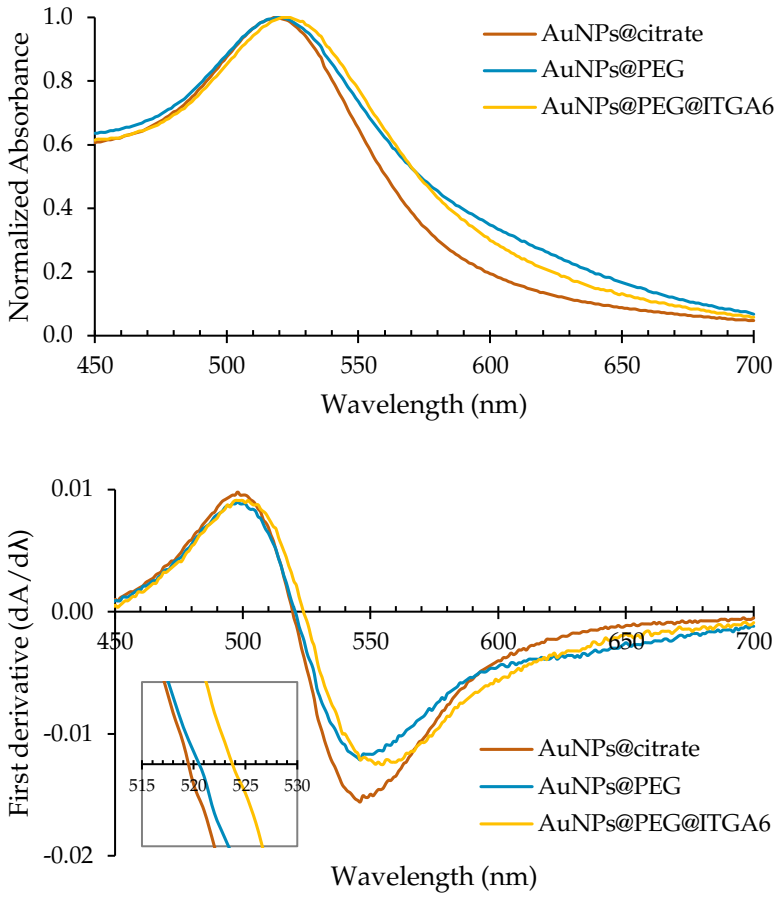

Figure 6. AuNPs UV-Vis Spectra. On top is displayed the absorption spectra of the synthetized AuNPs before and after each round of functionalization. Below is presented the first derivative spectra of the absorption spectra.

and AuNPs@ITGA6 of 40.44 ± 5.19 nm. Thus, it is visible an increase of average diameter from the naked to the 30% PEGylated AuNPs and from the 30% PEGylated to the DNA loaded AuNPs. The increase of hydrodynamic diameter has already been reported in the literature [240,277] and it is an indication that functionalization occurred. These data seem coherent with the data taken by the UV-Vis spectroscopy.

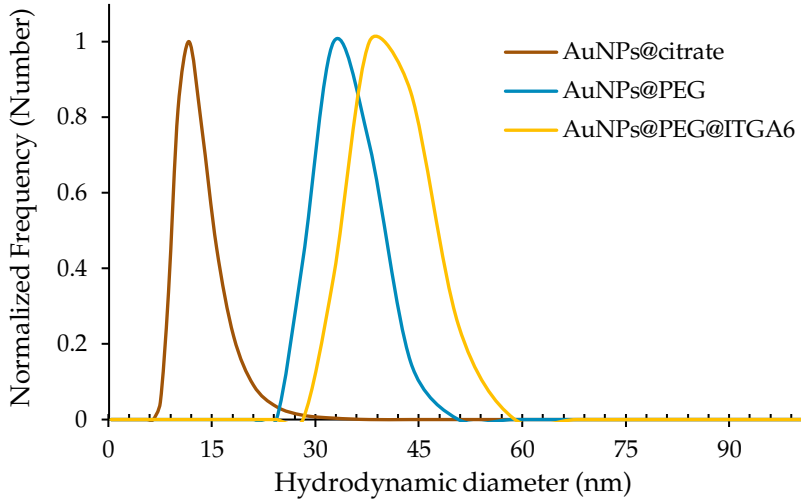

Figure 7. Particle size distribution curves. Hydrodynamic diameter distribution curves given by number obtained through DLS measurements for the synthetized AuNPs before and after each round of functionalization.

3.3. Primer Analysis and PCR Optimization

For the purpose of studying the *ITGA6* silencing efficiency by qPCR, it was required a pair of primers that specifically amplified *ITGA6* transcripts and a pair of primers capable of amplifying transcripts of a housekeeping gene. The sequences of the selected ITGA6 primers found in the literature[263] were the following:

Forward: 5'-GAG CTT TTG TGA TGG GCG ATT-3';

Reverse: 5'-CTC TCC ACC AAC TTC ATA AGG C-3'.

These sequences were submitted in the OligoAnalyzer[278] bioinformatic tool (https://www.idtdna.com/calc/analyzer) with the default settings to predict the primers secondary structures and to evaluate the potential for primers to interact with each other. They were also submitted in the Primer-BLAST[279] tool (https://www.ncbi.nlm.nih.gov/tools/primer-blast/) to calculate the primers properties and to check if they were target-specific. The results are exposed in the Table 2. As understandable by the table, the primers melting temperature (T_m) are very close ($\Delta T_m < 5$ °C) and the GC% of both primers are in the range of 40-55%. A low ΔT_m and a near 50% GC content will preclude one primer from base-pairing to the template more tenaciously than the other primer[280]. Concerning the self-dimer and heterodimer analysis, the values of ΔG associated with annealing of primers to the respective target regions are much more negative than the ΔG values for any of the secondary structures or primers complex predicted by the OligoAnalyzer program. Consequently, the likelihood of forming primer dimers is reduced. The Primer-BLAST results also showed ITGA6 primers have high specificity to *ITGA6* transcripts since no other amplification product was forecasted.

Table 2. ITGA6 primers properties.

Primer	T_m	GC%	ΔG(complementary sequence) (kcal/mol)	ΔG(most stable self-dimer) (kcal/mol)	ΔG(most stable heterodimer) (kcal/mol)
Forward	59.53 °C	47.62	-41.88	-6.34	-5.02
Reverse	58.73 °C	50.00	-40.28	-3.54	

Overall, these data suggest that the considered set of primers are capable of amplifying the target mRNA specifically. Moreover, the amplicon contains fragments of two adjacent exons spanning an intron with a length of 1593 nucleotides to avoid genomic DNA amplification.

After verifying the ITGA6 primers amplification capability *in silico* and knowing experimentally that GAPDH primers work, the RT-qPCR conditions were optimized and are detailed in the Table 1. The amplicon size for GAPDH primers is 226 bps, while for ITGA6 primers the amplicon size is 211 bps. The selected method for the relative quantification of *ITGA6* mRNA was the $2^{-\Delta\Delta Ct}$ method[264], since it was confirmed the amplification efficiencies are the same (Δefficiency < 5%). The typical profile of an amplification curve acquired for the

relative qualification of *ITGA6* transcripts is exposed in the Figure 8.A for GAPDH and in the Figure 8.B for ITGA6. The threshold line was set at 0.1. For each sample, it was assessed the presence of the right PCR product by analysing the melting curves and verifying the melting temperature (Figure 8.C for GAPDH and Figure 8.D for ITGA6) and by determining the size of the PCR product through agarose gel electrophoresis (Figure 8.E and Figure 8.F). In the image, melting curves and agarose gels show that both set of primers amplify its targets without amplifying unspecific products, an important factor to consider in qPCR.

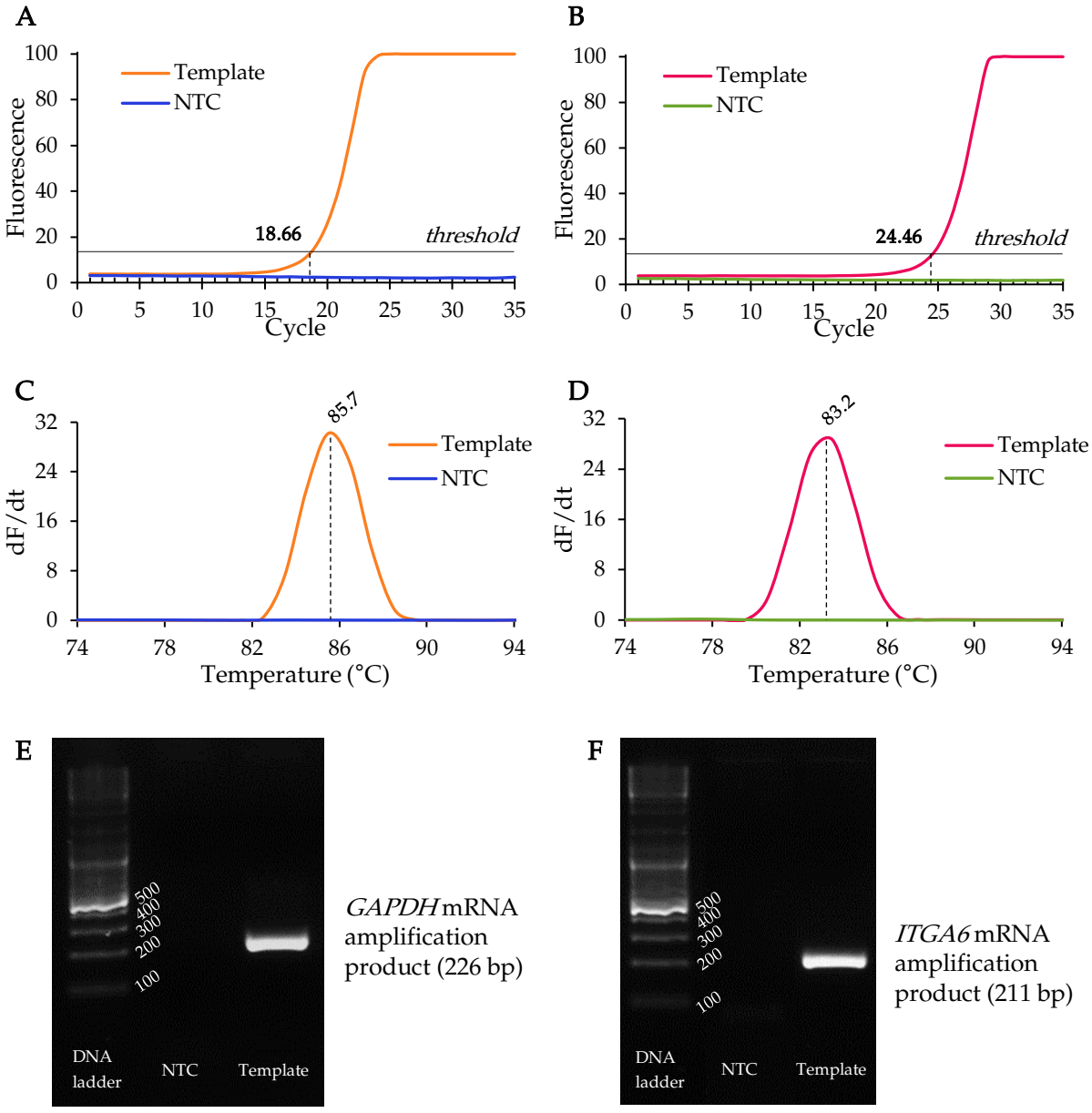

Figure 8. Specific PCR amplification of *GAPDH* and *ITGA6* RNAs applying optimized conditions. 10 ng of total RNA was reverse transcribed and amplified by one-step RT-qPCR. Typical amplification curves obtained employing the GAPDH **(A)** and ITGA6 **(B)** set of primers. The threshold was set at 0.1. Reaction products were analyzed by its melting curves [GAPDH – **(C)**; ITGA6 – **(D)**] and were separated on a 2% agarose gel [GAPDH – **(E)**; ITGA6 – **(F)**]. Template – Sample with RNA template; NTC – No template control.

3.4. *ITGA6* silencing

ITGA6 silencing efficacy was evaluated at the RNA level using RT-qPCR, at the protein level by western blot and through an experiment designed to detect phenotypic changes between cells treated with the Au-nanoconjugate and untreated cells.

3.4.1. RT-qPCR

ITGA6 relative expression was assessed by RT-qPCR analysis (Figure 9). 6, 14, 24, 48 and 72 h were the exposure times tested. By the bar plot analysis, it is possible to conclude that the maximum silencing event takes place at 48 h of exposure to 0.19 nM AuNPs@PEG@ITGA6 (39% silencing). Interestingly, the same exposure time was reported by Golbert et al. applying the same antisense binding sequence, although resorting to siRNA silencing[267]. The same authors also describe a 70-80% reduction of *ITGA6* mRNA[267]. The results disparity can be assignable to a) different cell lines (they used human thymic epithelial cells), b) different silencing mechanisms (siRNA vs ASO), c) influence of AuNPs, d) utilization of siRNAs combination (they combine 3 different siRNAs to enhance silencing) and e) the concentration of functionalized AuNPs can be further optimized. After 72 h, *ITGA6* expression is completely restored, fact possibly attributable to oligonucleotide degradation and/or cell expansion over time, which increases the number of cells per nanoparticle applied in cell medium[245,277]. These results indicate that treatment with the designed nanoconjugates provide efficient gene silencing.

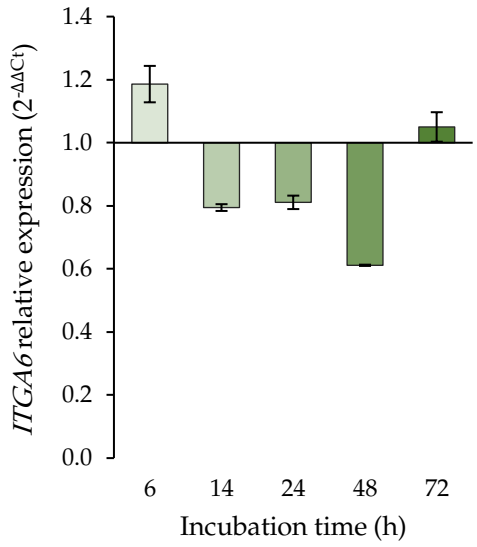

Figure 9. *ITGA6* silencing curve. *ITGA6* mRNA relative expression after treatment of MDA-MB-231 cells with AuNPs@PEG@ITGA6. Data were normalized to *GAPDH* and then to cells exposed to AuNPs@PEG. Error bars represent the standard error of the mean of at least two independent experiments. Error bars represent the standard error of the mean of two independent experiments. Ct – cycle threshold.

3.4.2. Western Blot

Differences in *ITGA6* expression were then determined at the protein level (Figure 10). Since ITGA6 is the only binding partner of ITGB4[281], the latter was also quantified to assess the impact of *ITGA6* downregulation in integrin $\alpha_6\beta_4$. After treatment with 0.19 nM AuNPs@PEG@ITGA6, ITGA6 protein expression decayed 22% and ITGB4 decreased 26%, comparing to PEGylated AuNPs alone. The divergence between the 39% silencing noted at

the RNA level and the 26% silencing at the protein level may derive from a delay between gene silencing and protein expression[277]. It is also visible a reduction of integrin $\alpha_6\beta_4$ protein expression (roughly 24%) upon addition of PEGylated nanoparticles without ASO that may be associated to endocytosis- and recycling-mediated integrin turnover, driven by intense endocytic internalization of AuNPs[282,283]. ITGB4 protein levels were shown to depend on the heterodimer formation with the ITGA6 subunit. These data prove that silencing efficacy occurred at the gene expression level, which was translated to protein level.

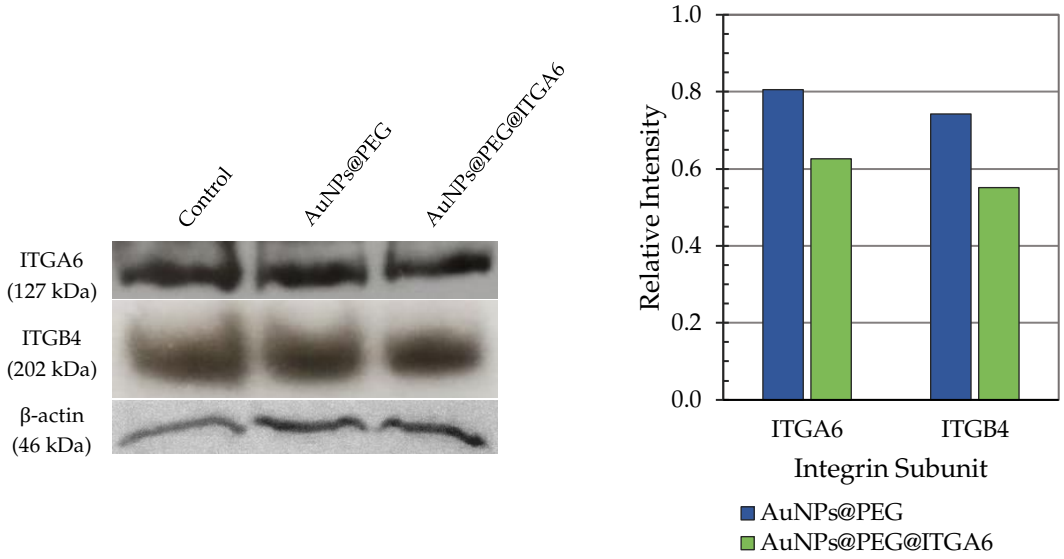

Figure 10. ITGA6 and ITGB4 relative quantification by western blot. ITGA6 (127 kDa) and ITGB4 (202 kDa) protein quantifications were performed via western blotting on MDA-MB-231 cell extracts after 48 h exposure to 0.19 nM AuNPs@PEG@ITGA6. Values were normalized against β-actin (42 kDa) and to the control condition. It was used one biological replicate.

3.4.3. Attachment Assay

To investigate whether the silencing of integrin $\alpha_6\beta_4$ translates itself into a phenotypical change, an attachment assay was conducted (Figure 11). Concretely, through this assay it was tested if decreasing integrin $\alpha_6\beta_4$ expression caused reduced cell adhesion. After 48 h of exposition to Au-nanoconjugates, cells were dissociated, transferred to new culture plates and left to adhere for 5 h. After medium removal, cells were counted. It seems to exist a slight decline of 13% in adhesion capability of cells treated with the antisense DNA-loaded AuNPs using the proportion AuNP:cell applied in the RT-qPCR and western blot analysis (5.9×10^8:1). The weak detachment event may be understood by the existence of an integrin with redundant functions. Integrins $\alpha_6\beta_1$, $\alpha_6\beta_4$ and $\alpha_3\beta_1$ play a crucial role on epithelial cells attachment to the BM by recognizing the COOH-terminal globular domains of the laminin α-subunit[284]. The successful *ITGA6* knockdown may not be sufficient to affect cell adhesion because synthesis of integrin $\alpha_3\beta_1$ is not inhibited and can attenuate the phenotypic effect, since it has a redundant function. Even so, it was made a second experience to attempt a pronunciation of the detachment effect, where it was raised the proportion of AuNP:cell to 2.3×10^{10}:1. This time cell adhesion capability diminished by 38%. In this sense, results point that

the silencing event provokes a reduction of the cell adhesion capability and corroborates that functionalized AuNPs have gene silencing activity. Due to time constraints, it was not possible to proceed with the study, but more experiences are required to make a statistical analysis and to take valid conclusions.

In general, the information taken by the techniques put into practice in this section suggest that the formulated AuNPs@PEG@ITGA6 are endowed with gene silencing activity. The *ITGA6* knockdown ultimately result in lower integrin $\alpha_6\beta_4$ protein expression and consequent lower adherence of MDA-MB-231 cells.

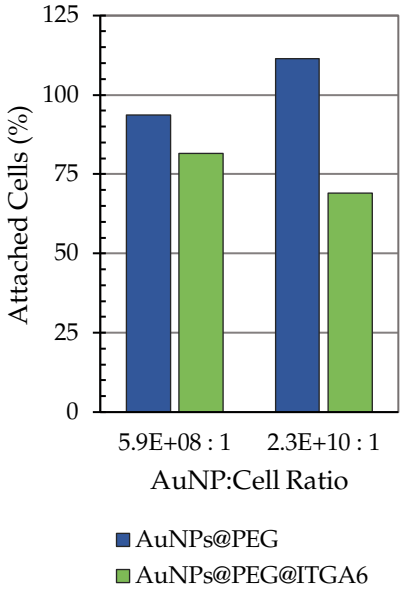

Figure 11. Attachment assay. MDA-MB-231 cells treated with AuNPs@PEG and AuNPs@PEG@ITGA6 were left to adhere during 5 h. Thereafter, cells attached to the culture plate were counted. Values were normalized to the control condition. It was used one biological replicate.

| 4.

CONCLUSIONS AND FUTURE PERSPECTIVES

An ASO was designed to target *ITGA6* mRNAs. The silence efficacy was firstly evaluated by doing an analysis *in silico*. This analysis showed that the ASO-target hybridization was thermodynamically favoured and that the target binding sequence had low probability of pairing with other regions of the *ITGA6* transcript. The ASO specificity was also confirmed using the BLAST bioinformatic tool. Then, AuNPs with an average diameter of 14 nm were PEGylated to increase stability in biological environment and further functionalized with the produced ASO. Characterization of Au-nanoconjugates showed that each functionalization round occurred and nanoparticles were stable in solution. MDA-MB-231 cells were challenged with the Au-nanoconjugates using different exposure times. The deepest silencing event was observed at 48 h of incubation with 39% silencing in comparison to PEGylated AuNPs. The western blot analysis revealed that decreasing *ITGA6* expression resulted not only in reduced ITGA6 synthesis but also in diminished ITGB4 protein levels, 22% and 26% respectively. Therefore, by downregulating ITGA6 subunit, it is postulated that the assembly of integrin $\alpha_6\beta_4$ is inhibited. Lastly, to understand if the cell adhesion capability was affected by lower levels of integrin $\alpha_6\beta_4$, it was conducted an attachment assay. Cells treated with DNA-loaded AuNPs seem to possess less adhesion properties but more experiences are needed to assess if there is statistical difference between these two groups. Overall, these results demonstrate that the developed Au-nanoconjugates can efficiently reduce *ITGA6* expression, which translates into lower protein levels. By inhibiting integrin $\alpha_6\beta_4$ synthesis, this nanoformulation exhibits great potential to prevent the transport of these integrins by exosomes, and consequently to cease lung organotropism of the breast cancer cells-derived EVs. In the future, this strategy may be an attractive tool to fight lung metastasis.

It remained to be addressed whether the silencing effect can be enhanced by changing the AuNP:cell ratio. In this sense, testing other proportions may be advantageous. Moreover, the attachment assay can be improved with a previous step consisting on coating the wells with laminin (ligand recognized by integrins $\alpha_6\beta_1$ and $\alpha_6\beta_4$). Further studies include also the evaluation of the integrin abundance in exosomes derived from untreated and AuNPs@PEG@ITGA6-treated cells. Lastly, to try to understand if the silenced exosome integrins halt exosome uptake and consequent PMN formation, incubation of human lung

fibroblasts and bronchial epithelial cells with exosomes exposed to the nanoconjugate are needed. For that to happen, isolated exosomes can be labelled with a membrane fluorescent dye, like PKH67, and the uptake tracked by fluorescence microscopy upon incubation with lung cells.

REFERENCES

1. Ferlay J, Ervik M, Lam F, et al. Global Cancer Observatory: Cancer Today. Accessed October 20, 2021. https://gco.iarc.fr/today
2. Sung H, Ferlay J, Siegel RL, et al. Global Cancer Statistics 2020: GLOBOCAN Estimates of Incidence and Mortality Worldwide for 36 Cancers in 185 Countries. *CA Cancer J Clin*. 2021;71(3):209-249. doi:10.3322/caac.21660
3. Mattiuzzi C, Lippi G. Current Cancer Epidemiology. *J Epidemiol Glob Health*. 2019;9(4):217-222.
4. Dillekås H, Rogers MS, Straume O. Are 90% of deaths from cancer caused by metastases? *Cancer Med*. 2019;8(12):5574-5576. doi:10.1002/cam4.2474
5. Gupta GP, Massagué J. Cancer Metastasis: Building a Framework. *Cell*. 2006;127(4):679-695. doi:10.1016/j.cell.2006.11.001
6. Hanahan D, Weinberg RA. The Hallmarks of Cancer. *Cell*. 2000;100:57-70.
7. Fentiman IS, Fourquet A, Hortobagyi GN. Male breast cancer. *Lancet*. 2006;367(9510):595-604. doi:10.1016/S0140-6736(06)68226-3
8. Harbeck N, Penault-Llorca F, Cortes J, et al. Breast cancer. *Nat Rev Dis Prim*. 2019;5(66). doi:10.1038/s41572-019-0111-2
9. Fragomeni SM, Sciallis A, Jeruss JS. Molecular Subtypes and Local-Regional Control of Breast Cancer. *Surg Oncol Clin N Am*. 2018;27(1):95-120. doi:10.1016/j.soc.2017.08.005
10. Waks AG, Winer EP. Breast Cancer Treatment: A Review. *JAMA - J Am Med Assoc*. 2019;321(3):288-300. doi:10.1001/jama.2018.19323
11. O'Shaughnessy J. Extending Survival with Chemotherapy in Metastatic Breast Cancer. *Oncologist*. 2005;10(S3):20-29. doi:10.1634/theoncologist.10-90003-20
12. Cardoso F, Spence D, Mertz S, et al. Global analysis of advanced/metastatic breast cancer: Decade report (2005–2015). *Breast*. 2018;39:131-138. doi:10.1016/j.breast.2018.03.002
13. Lim B, Hortobagyi GN. Current challenges of metastatic breast cancer. *Cancer Metastasis Rev*. 2016;35(4):495-514. doi:10.1007/s10555-016-9636-y
14. Jones SE. Metastatic breast cancer: The treatment challenge. *Clin Breast Cancer*. 2008;8(3):224-233. doi:10.3816/CBC.2008.n.025
15. Arnedos M, Vicier C, Loi S, et al. Precision medicine for metastatic breast cancer-limitations and solutions. *Nat Rev Clin Oncol*. 2015;12(12):693-704. doi:10.1038/nrclinonc.2015.123
16. Zardavas D, Baselga J, Piccart M. Emerging targeted agents in metastatic breast cancer. *Nat Rev Clin Oncol*. 2013;10(4):191-210. doi:10.1038/nrclinonc.2013.29

17. Nordling C. A new theory on the cancer-inducing mechanism. *Br J Cancer*. 1953;7:68-72.

18. John Cairns. Mutation selection and the natural history of cancer. *Nature*. 1975;255:197-200.

19. Nowell P. C. The clonal evolution of tumor cell populations. *Science*. 1976;194:23-28.

20. Greaves M, Maley CC. Clonal evolution in cancer. *Nature*. 2012;481:306-312. doi:10.1038/nature10762

21. Chaffer CL, Weinberg RA. How does multistep tumorigenesis really proceed? *Cancer Discov*. 2015;5(1):22-24. doi:10.1158/2159-8290.CD-14-0788

22. Fearon ER, Vogelstein B. A Genetic Model for Colorectal Tumorigenesis. *Cell*. 1989;61:759-767.

23. Vogei B, Kinzi TW. The multistep nature of cancer. *Trends Genet*. 1993;9(4):138-141.

24. Lapidot T, Sirard C, Vormoor J, et al. A cell initiating human acute myeloid leukaemia after transplantation into SCID mice. *Nature*. 1994;367:645-648. doi:10.1038/367645a0

25. Lee J, Olofsson BA, Mwidau A, et al. Prospective identification of tumorigenic breast cancer cells. *PNAS*. 2003;100(7):3983-3988.

26. Bonnet D, Dick J. Human acute myeloid leukemia is organized as a hierarchy that originates from a primitive hematopoietic cell. *Nat Med*. 1997;3(7):730-737.

27. Reya T, Morrison SJ, Clarke MF, Weissman IL. Stem cells, cancer, and cancer stem cells. *Nature*. 2001;414:105-111.

28. Dick JE. Stem cell concepts renew cancer research. *Blood*. 2008;112(13):4793-4807. doi:10.1182/blood-2008-08-077941.

29. Wang JCY, Dick JE. Cancer stem cells: Lessons from leukemia. *Trends Cell Biol*. 2005;15(9):494-501. doi:10.1016/j.tcb.2005.07.004

30. Walcher L, Kistenmacher A, Suo H, Kitte R, Dluczek S, Kossatz-boehlert U. Cancer Stem Cells - Origins and Biomarkers : Perspectives for Targeted Personalized Therapies. *Front Immunol*. 2020;11(1280). doi:10.3389/fimmu.2020.01280

31. Nassar D, Blanpain C. Cancer Stem Cells: Basic Concepts and Therapeutic Implications. *Annu Rev Pathol Mech Dis*. 2016;11:47-76. doi:10.1146/annurev-pathol-012615-044438

32. Clarke MF, Dick JE, Dirks PB, et al. Cancer stem cells - Perspectives on current status and future directions: AACR workshop on cancer stem cells. *Cancer Res*. 2006;66(19):9339-9344. doi:10.1158/0008-5472.CAN-06-3126

33. Clarke MF, Fuller M. Stem Cells and Cancer : Two Faces of Eve. *Cell*. 2006;124(6):1111-1115. doi:10.1016/j.cell.2006.03.011

34. Visvader JE. Cells of origin in cancer. *Nature*. 2011;469:314-322. doi:10.1038/nature09781

35. Shackleton M, Quintana E, Fearon ER, Morrison SJ. Heterogeneity in Cancer : Cancer Stem Cells versus Clonal Evolution. *Cell*. 2009;138:822-829. doi:10.1016/j.cell.2009.08.017

36. Kreso A, Dick JE. Evolution of the cancer stem cell model. *Cell Stem Cell*. 2014;14(3):275-291. doi:10.1016/j.stem.2014.02.006

37. Tang DG. Understanding cancer stem cell heterogeneity and plasticity. *Cell Res*. 2012;22(3):457-472. doi:10.1038/cr.2012.13

38. Toh TB, Lim JJ, Chow EK. Epigenetics in cancer stem cells. *Mol Cancer*. 2017;16(29).

doi:10.1186/s12943-017-0596-9

39. Chaffer CL, Marjanovic ND, Lee T, et al. Poised Chromatin at the ZEB1 Promoter Enables Breast Cancer Cell Plasticity and Enhances Tumorigenicity. *Cell*. 2013;154(1):61-74. doi:10.1016/j.cell.2013.06.005
40. Feinberg AP, Ohlsson R, Henikoff S. The epigenetic progenitor origin of human cancer. *Nat Rev Genet*. 2006;7:21-33. doi:10.1038/nrg1748
41. Sharma S, Kelly TK, Jones PA. Epigenetics in cancer. *Carcinogenesis*. 2010;31(1):27-36. doi:10.1093/carcin/bgp220
42. Batlle E, Clevers H. Cancer stem cells revisited. *Nat Med*. 2017;23(10):1124-1134. doi:10.1038/nm.4409
43. Wang M, Zhao J, Zhang L, et al. Role of tumor microenvironment in tumorigenesis. *J Cancer*. 2017;8(5):761-773. doi:10.7150/jca.17648
44. Tabassum DP, Polyak K. Tumorigenesis: It takes a village. *Nat Rev Cancer*. 2015;15(8):473-483. doi:10.1038/nrc3971
45. Hanahan D, Weinberg RA. Hallmarks of cancer: The next generation. *Cell*. 2011;144(5):646-674. doi:10.1016/j.cell.2011.02.013
46. Evan GI, Vousden KH. Proliferation, cell cycle and apoptosis in cancer. *Nature*. 2001;411:342-348. doi:10.1038/35077213
47. Witsch E, Sela M, Yarden Y. Roles for Growth Factors in Cancer Progression. *Physiology*. 2010;25(2):85-101. doi:10.1152/physiol.00045.2009
48. Zhao M, Jung Y, Jiang Z, Svensson KJ. Regulation of Energy Metabolism by Receptor Tyrosine Kinase Ligands. *Front Physiol*. 2020;11(354). doi:10.3389/fphys.2020.00354
49. Saraon P, Pathmanathan S, Snider J, Lyakisheva A, Wong V, Stagljar I. Receptor tyrosine kinases and cancer: oncogenic mechanisms and therapeutic approaches. *Oncogene*. 2021;40(24):4079-4093. doi:10.1038/s41388-021-01841-2
50. Takeuchi K, Ito F. Receptor tyrosine kinases and targeted cancer therapeutics. *Biol Pharm Bull*. 2011;34(12):1774-1780. doi:10.1248/bpb.34.1774
51. Paul MK, Mukhopadhyay AK. Tyrosine kinase – Role and significance in Cancer. *Int J Med Sci*. 2004;1(2):101-115. doi:10.7150/ijms.1.101
52. DeBerardinis RJ, Lum JJ, Hatzivassiliou G, Thompson CB. The Biology of Cancer: Metabolic Reprogramming Fuels Cell Growth and Proliferation. *Cell Metab*. 2008;7(1):11-20. doi:10.1016/j.cmet.2007.10.002
53. Giacinti C, Giordano A. RB and cell cycle progression. *Oncogene*. 2006;25(38):5220-5227. doi:10.1038/sj.onc.1209615
54. Huang HJS, Yee JK, Shew JY, et al. Suppression of the neoplastic phenotype by replacement of the rb gene in human cancer cells. *Science*. 1988;242(4885):1563-1566. doi:10.1126/science.3201247
55. Lane DP. P53, Guardian of the Genome. *Nature*. 1992;358:15-16. doi:10.1038/358015a0
56. Wynford-Thomas D. p53, the Cellular Gatekeeper for Growth and Division. *Eur J Cancer Part A*. 1997;33(5):716-726. doi:10.1016/S0959-8049(97)00064-6
57. Green DR, Chipuk JE. p53 and Metabolism: Inside the TIGAR. *Cell*. 2006;126(1):30-32. doi:10.1016/j.cell.2006.06.032
58. Reed JC. Bcl-2 Family Proteins. *Oncogene*. 1998;17:3225–3236.
59. Elmore S. Apoptosis: A Review of Programmed Cell Death. *Toxicol Pathol*.

2007;35(4):495-516. doi:10.1080/01926230701320337

60. Ouyang L, Shi Z, Zhao S, et al. Programmed cell death pathways in cancer: A review of apoptosis, autophagy and programmed necrosis. *Cell Prolif*. 2012;45(6):487-498. doi:10.1111/j.1365-2184.2012.00845.x

61. McIlwain DR, Berger T, Mak TW. Caspase functions in cell death and disease. *Cold Spring Harb Perspect Biol*. 2015;7(4). doi:10.1101/cshperspect.a026716

62. Harley CB. Telomere loss: mitotic clock or genetic time bomb? *Mutat Res*. 1991;256(2-6):271-282. doi:10.1016/0921-8734(91)90018-7

63. Counter CM, Avilion AA, Lefeuvre CE, et al. Telomere shortening associated with chromosome instability is arrested in immortal cells which express telomerase activity. *EMBO J*. 1992;11(5):1921-1929. doi:10.1002/j.1460-2075.1992.tb05245.x

64. Shay JW, Wright WE. Senescence and immortalization: Role of telomeres and telomerase. *Carcinogenesis*. 2005;26(5):867-874. doi:10.1093/carcin/bgh296

65. Harley CB, Kim NW, Prowse KR, et al. Telomerase, cell immortality, and cancer. *Cold Spring Harb Symp Quant Biol*. 1994;59:307-315. doi:10.1101/SQB.1994.059.01.035

66. Hahn WC, Stewart SA, Brooks MW, et al. Inhibition of telomerase limits the growth of human cancer cells. *Nat Med*. 1999;5(10):1164-1170. doi:10.1038/13495

67. Recagni M, Bidzinska J, Zaffaroni N, Folini M. The role of alternative lengthening of telomeres mechanism in cancer: Translational and therapeutic implications. *Cancers (Basel)*. 2020;12(4):1-15. doi:10.3390/cancers12040949

68. Nishida N, Yano H, Nishida T, Kamura T, Kojiro M. Angiogenesis in cancer. *Vasc Health Risk Manag*. 2006;2(3):213-219. doi:10.2147/vhrm.2006.2.3.213

69. Aguilar-Cazares D, Chavez-Dominguez R, Carlos-Reyes A, Lopez-Camarillo C, Hernadez de la Cruz ON, Lopez-Gonzalez JS. Contribution of Angiogenesis to Inflammation and Cancer. *Front Oncol*. 2019;9(1399). doi:10.3389/fonc.2019.01399

70. Carmeliet P. VEGF as a key mediator of angiogenesis in cancer. *Oncology*. 2005;69(SUPPL. 3):4-10. doi:10.1159/000088478

71. Bergers G, Benjamin LE. Tumorigenesis and the angiogenic switch. *Nat Rev Cancer*. 2003;3(6):401-410. doi:10.1038/nrc1093

72. Folkman J. Angiogenesis in cancer, vascular, rheumatoid and other disease. *Nat Med*. 1995;1:27-30. doi:10.1038/nm0195-27

73. Warburg O, Wind F, Negelein E. The metabolim of tumors in the body. *J Gen Physiol*. 1927;8(6):519-530.

74. DeBerardinis RJ, Chandel NS. We need to talk about the Warburg effect. *Nat Metab*. 2020;2(2):127-129. doi:10.1038/s42255-020-0172-2

75. Wong CC, Qian Y, Yu J. Interplay between epigenetics and metabolism in oncogenesis: Mechanisms and therapeutic approaches. *Oncogene*. 2017;36(24):3359-3374. doi:10.1038/onc.2016.485

76. De Berardinis RJ, Chandel NS. Fundamentals of cancer metabolism. *Sci Adv*. 2016;2(5):e1600200. doi:10.1126/sciadv.1600200

77. Zheng J. Energy metabolism of cancer: Glycolysis versus oxidative phosphorylation (review). *Oncol Lett*. 2012;4(6):1151-1157. doi:10.3892/ol.2012.928

78. Pavlova NN, Thompson CB. The Emerging Hallmarks of Cancer Metabolism. *Cell Metab*. 2016;23(1):27-47. doi:10.1016/j.cmet.2015.12.006

79. Ehrlich P. Ueber den jetzigen Stand der Karzinomforschung. *Ned Tijdschr Geneeskd*. 1909;5:273-290.

80. Burnet M. Cancer-A Biological Approach. III. Viruses Associated With Neoplastic Conditions. *Br Med J*. 1957;1(5023):841-847. doi:10.1136/bmj.1.5023.841

81. Burnet FM. The Concept of Immunological Surveillance. *Progr exp Tumor Res*. 1970;13:1-27.

82. Burnet M. Immunlogical Factors in the Proccess of Carcinogenesis. *Brit med Bull*. 1964;20:154-158.

83. Thomas L. On immunosurveillance in human cancer. *Yale J Biol Med*. 1982;55(3-4):329-333.

84. Dunn GP, Old LJ, Schreiber RD. The immunobiology of cancer immunosurveillance and immunoediting. *Immunity*. 2004;21(2):137-148. doi:10.1016/j.immuni.2004.07.017

85. Ostrand-Rosenberg S. Immune Surveillance: A Balance Between Pro- and Anti-tumor Immunity. *Curr Opin Genet Dev*. 2008;18(1):11-18. doi:10.1016/j.gde.2007.12.007.Immune

86. Ribatti D. The concept of immune surveillance against tumors: The first theories. *Oncotarget*. 2017;8(4):7175-7180. www.impactjournals.com/oncotarget/

87. Stutman O. Tumor development after 3-methylcholanthrene in immunologically deficient athymic-nude mice. *Science*. 1974;183(4124):534-536. http://www.sciencemag.org/cgi/doi/10.1126/science.134.3478.527

88. Dunn GP, Bruce AT, Ikeda H, Old LJ, Schreiber RD. Cancer immunoediting: From immunosurveillance to tumor escape. *Nat Immunol*. 2002;3(11):991-998. doi:10.1038/ni1102-991

89. Dunn GP, Old LJ, Schreiber RD. The three Es of cancer immunoediting. *Annu Rev Immunol*. 2004;22(4):329-360. doi:10.1146/annurev.immunol.22.012703.104803

90. Mittal D, Gubin MM, Schreiber RD, Smyth MJ. New insights into cancer immunoediting and its three component phases—elimination, equilibrium and escape. Current opinion in immunology. 2014 Apr 1;27:16-25. *Curr Opin Immunol*. 2014;27:16-25. doi:10.1016/j.coi.2014.01.004.New

91. Talmadge JE, Fidler IJ. AACR centennial series: The biology of cancer metastasis: Historical perspective. *Cancer Res*. 2010;70(14):5649-5669. doi:10.1158/0008-5472.CAN-10-1040

92. Fidler IJ. The pathogenesis of cancer metastasis: the 'seed and soil' hypothesis revisited. *Nat Rev Cancer*. 2003;3(6):453-458. doi:10.1038/nrc1098

93. Majidpoor J, Mortezaee K. Steps in metastasis: an updated review. *Med Oncol*. 2021;38:3. doi:10.1007/s12032-020-01447-w

94. Fares J, Fares MY, Khachfe HH, Salhab HA, Fares Y. Molecular principles of metastasis: a hallmark of cancer revisited. *Signal Transduct Target Ther*. 2020;5:28. doi:10.1038/s41392-020-0134-x

95. Valastyan S, Weinberg RA. Tumor metastasis: Molecular insights and evolving paradigms. *Cell*. 2011;147(2):275-292. doi:10.1016/j.cell.2011.09.024

96. Joyce JA, Pollard JW. Microenvironmental regulation of metastasis. *Nat Rev Cancer*. 2009;9(4):239-252. doi:10.1038/nrc2618

97. Chang J, Chaudhuri O. Beyond proteases: Basement membrane mechanics and cancer invasion. *J Cell Biol*. 2019;218(8):2456-2469. doi:10.1083/JCB.201903066

98. Curran S, Murray GI. Matrix metalloproteinases in tumour invasion and metastasis. *J Pathol*. 1999;189:300-308.

99. Kessenbrock K, Plaks V, Werb Z. Matrix Metalloproteinases: Regulators of the Tumor Microenvironment. *Cell*. 2010;141(1):52-67. doi:10.1016/j.cell.2010.03.015

100. Smith HA, Kang Y. The Metastasis-Promoting Roles of Tumor-Associated Immune Cells. *J Mol Med*. 2013;91(4):411-429. doi:10.1007/s00109-013-1021-5.The

101. Guo S, Deng CX. Effect of stromal cells in tumor microenvironment on metastasis initiation. *Int J Biol Sci*. 2018;14(14):2083-2093. doi:10.7150/ijbs.25720

102. Kitamura T, Qian B-Z, Pollard JW. Immune cell promotion of metastasis. *Nat Rev Immunol*. 2015;15(2):73-86. doi:10.1038/nri3789.Immune

103. Winkler J, Abisoye-Ogunniyan A, Metcalf KJ, Werb Z. Concepts of extracellular matrix remodelling in tumour progression and metastasis. *Nat Commun*. 2020;11(1):1-19. doi:10.1038/s41467-020-18794-x

104. Bussard KM, Mutkus L, Stumpf K, Gomez-Manzano C, Marini FC. Tumor-associated stromal cells as key contributors to the tumor microenvironment. *Breast Cancer Res*. 2016;18(1):1-11. doi:10.1186/s13058-016-0740-2

105. Thiery JP, Acloque H, Huang RYJ, Nieto MA. Epithelial-Mesenchymal Transitions in Development and Disease. *Cell*. 2009;139(5):871-890. doi:10.1016/j.cell.2009.11.007

106. Yang J, Antin P, Berx G, et al. Guidelines and definitions for research on epithelial–mesenchymal transition. *Nat Rev Mol Cell Biol*. 2020;21(6):341-352. doi:10.1038/s41580-020-0237-9

107. Chiang SPH, Cabrera RM, Segall JE. Tumor cell intravasation. *Am J Physiol - Cell Physiol*. 2016;311(1):C1-C14. doi:10.1152/ajpcell.00238.2015

108. Zavyalova M V., Denisov E V., Tashireva LA, et al. Intravasation as a Key Step in Cancer Metastasis. *Biochem*. 2019;84(7):762-772. doi:10.1134/S0006297919070071

109. Gligorijevic B, Wyckoff J, Yamaguchi H, Wang Y, Roussos ET, Condeelis J. N-WASP-mediated invadopodium formation is involved in intravasation and lung metastasis of mammary tumors. *J Cell Sci*. 2012;125(3):724-734. doi:10.1242/jcs.092726

110. Wyckoff JB, Wang Y, Lin EY, et al. Direct visualization of macrophage-assisted tumor cell intravasation in mammary tumors. *Cancer Res*. 2007;67(6):2649-2656. doi:10.1158/0008-5472.CAN-06-1823

111. Strilic B, Offermanns S. Intravascular Survival and Extravasation of Tumor Cells. *Cancer Cell*. 2017;32(3):282-293. doi:10.1016/j.ccell.2017.07.001

112. Wirtz D, Konstantopoulos K, Searson PC. The physics of cancer: The role of physical interactions and mechanical forces in metastasis. *Nat Rev Cancer*. 2011;11(7):512-522. doi:10.1038/nrc3080

113. Follain G, Herrmann D, Harlepp S, et al. Fluids and their mechanics in tumour transit: shaping metastasis. *Nat Rev Cancer*. 2020;20(2):107-124. doi:10.1038/s41568-019-0221-x

114. Goetz JG. Metastases go with the flow. *Science*. 2018;362(6418):999-1000. doi:10.1126/science.aat9100

115. Pross HF, Lotzova E. Role of Natural Killer Cells In the Destruction of Circulating Tumor Emboli. *Nat Immun*. 1993;12(4-5):279-292.

116. Palumbo JS, Talmage KE, Massari J V., et al. Platelets and fibrin(ogen) increase metastatic potential by impeding natural killer cell-mediated elimination of tumor cells.

Blood. 2005;105(1):178-185. doi:10.1182/blood-2004-06-2272

117. Gay LJ, Felding-Habermann B. Contribution of platelets to tumour metastasis. *Nat Rev Cancer*. 2011;11(2):123-134. doi:10.1038/nrc3004

118. Theos AC, Martina A, Hurbain I, et al. Transendothelial Migration of Melanoma Cells Involves N-Cadherin-mediated Adhesion and Activation of the beta-Catenin Signaling Pathway. *Mol Biol Cell*. 2005;16(9):4386-4397. doi:10.1091/mbc.E05

119. Massagué J, Obenauf AC. Metastatic colonization by circulating tumour cells. *Nature*. 2016;529:298-306. doi:10.1038/nature17038

120. Smyth MJ, Thia KY, Cretney E, et al. Perforin is a major contributor to NK cell control of tumor metastasis. *J Immunol*. 1999;162:6658-6662.

121. Eyles J, Puaux AL, Wang X, et al. Tumor cells disseminate early, but immunosurveillance limits metastatic outgrowth, in a mouse model of melanoma. *J Clin Invest*. 2010;120(6):2030-2039. doi:10.1172/JCI42002

122. Giancotti FG. Mechanisms governing metastatic dormancy and reactivation. *Cell*. 2013;155(4):750. doi:10.1016/j.cell.2013.10.029

123. Sosa MS, Bragado P, Aguirre-Ghiso JA. Mechanisms of disseminated cancer cell dormancy: An awakening field. *Nat Rev Cancer*. 2014;14(9):611-622. doi:10.1038/nrc3793

124. Holmgren L, O'reilly MS, Folkman J. Dormancy of micrometastases: Balanced proliferation and apoptosis in the presence of angiogenesis suppression. *Nat Med*. 1995;1(2):149-153. doi:10.1038/nm0295-149

125. Aguirre-Ghiso JA. Models, mechanisms and clinical evidence for cancer dormancy. *Nat Rev Cancer*. 2007;7(11):834-846. doi:10.1038/nrc2256

126. Klein CA. Cancer progression and the invisible phase of metastatic colonization. *Nat Rev Cancer*. 2020;20(11):681-694. doi:10.1038/s41568-020-00300-6

127. Malanchi I, Santamaria-Martínez A, Susanto E, et al. Interactions between cancer stem cells and their niche govern metastatic colonization. *Nature*. 2012;481:85-91. doi:10.1038/nature10694

128. Liu Y, Cao X. Characteristics and Significance of the Pre-metastatic Niche. *Cancer Cell*. 2016;30(5):668-681. doi:10.1016/j.ccell.2016.09.011

129. Paget S. Distribution of Secondary Growths in Cancer of the Breast. *Lancet*. 1889;8(2):98-101.

130. Wortzel I, Dror S, Kenific CM, Lyden D. Exosome-Mediated Metastasis: Communication from a Distance. *Dev Cell*. 2019;49(3):347-360. doi:10.1016/j.devcel.2019.04.011

131. Lobb RJ, Lima LG, Möller A. Exosomes: Key mediators of metastasis and pre-metastatic niche formation. *Semin Cell Dev Biol*. 2017;67:3-10. doi:10.1016/j.semcdb.2017.01.004

132. Guo Y, Ji X, Liu J, et al. Effects of exosomes on pre-metastatic niche formation in tumors. *Mol Cancer*. 2019;18:39. doi:10.1186/s12943-019-0995-1

133. Peinado H, Lavotshkin S, Lyden D. The secreted factors responsible for pre-metastatic niche formation: Old sayings and new thoughts. *Semin Cancer Biol*. 2011;21(2):139-146. doi:10.1016/j.semcancer.2011.01.002

134. Tlsty TD, Coussens LM. Tumor stroma and regulation of cancer development. *Annu Rev Pathol*. 2006;1:119-150. doi:10.1146/annurev.pathol.1.110304.100224

135. Whiteside TL. The tumor microenvironment and its role in promoting tumor growth.

Oncogene. 2008;27(45):5904-5912. doi:10.1038/onc.2008.271

136. Balkwill FR, Capasso M, Hagemann T. The tumor microenvironment at a glance. *J Cell Sci*. 2012;125(23):5591-5596. doi:10.1242/jcs.116392

137. Grivennikov SI, Greten FR, Karin M. Immunity, Inflammation, and Cancer. *Cell*. 2010;140(6):883-899. doi:10.1016/j.cell.2010.01.025

138. Mantovani A, Allavena P, Sica A, Balkwill F. Cancer-related inflammation. *Nature*. 2008;454:436-444. doi:10.1038/nature07205

139. Greten FR, Grivennikov SI. Inflammation and Cancer: Triggers, Mechanisms, and Consequences. *Immunity*. 2019;51(1):27-41. doi:10.1016/j.immuni.2019.06.025

140. Dvorak HF. Tumors: wounds that do not heal. Similarities between tumor stroma generation and wound healing. *N Engl J Med*. 1986;315(26):1650-1659. doi:10.1056/NEJM198612253152606

141. Sahai E, Astsaturov I, Cukierman E, et al. A framework for advancing our understanding of cancer-associated fibroblasts. *Nat Rev Cancer*. 2020;20(3):174-186. doi:10.1038/s41568-019-0238-1

142. Kalluri R, LeBleu VS. The biology, function, and biomedical applications of exosomes. *Science*. 2020;367(6478). doi:10.1126/science.aau6977

143. Roma-Rodrigues C, Fernandes AR, Baptista PV. Exosome in tumour microenvironment: Overview of the crosstalk between normal and cancer cells. *Biomed Res Int*. 2014;2014:179486. doi:10.1155/2014/179486

144. Mashouri L, Yousefi H, Aref AR, Ahadi AM, Molaei F, Alahari SK. Exosomes: Composition, biogenesis, and mechanisms in cancer metastasis and drug resistance. *Mol Cancer*. 2019;18:75. doi:10.1186/s12943-019-0991-5

145. Van Niel G, D'Angelo G, Raposo G. Shedding light on the cell biology of extracellular vesicles. *Nat Rev Mol Cell Biol*. 2018;19(4):213-228. doi:10.1038/nrm.2017.125

146. Colombo M, Raposo G, Théry C. Biogenesis, secretion, and intercellular interactions of exosomes and other extracellular vesicles. *Annu Rev Cell Dev Biol*. 2014;30:255-289. doi:10.1146/annurev-cellbio-101512-122326

147. Hutagalung AH, Novick PJ. Role of Rab GTPases in membrane traffic and cell physiology. *Physiol Rev*. 2011;91:119-149. doi:10.1152/physrev.00059.2009

148. Blanc L, Vidal M. New insights into the function of Rab GTPases in the context of exosomal secretion. *Small GTPases*. 2018;9(1-2):95-106. doi:10.1080/21541248.2016.1264352

149. Wandinger-Ness A, Zerial M. Rab proteins and the compartmentalization of the endosomal system. *Cold Spring Harb Perspect Biol*. 2014;6(11):a022616. doi:10.1101/cshperspect.a022616

150. Hessvik NP, Llorente A. Current knowledge on exosome biogenesis and release. *Cell Mol Life Sci*. 2018;75(2):193-208. doi:10.1007/s00018-017-2595-9

151. Raposo G, Stoorvogel W. Extracellular vesicles: Exosomes, microvesicles, and friends. *J Cell Biol*. 2013;200(4):373-383. doi:10.1083/jcb.201211138

152. Peinado H, Zhang H, Matei IR, et al. Pre-metastatic niches: Organ-specific homes for metastases. *Nat Rev Cancer*. 2017;17(5):302-317. doi:10.1038/nrc.2017.6

153. Zeng Z, Li Y, Pan Y, et al. Cancer-derived exosomal miR-25-3p promotes pre-metastatic niche formation by inducing vascular permeability and angiogenesis. *Nat Commun*. 2018;9:5395. doi:10.1038/s41467-018-07810-w

154. Goulet CR, Bernard G, Tremblay S, Chabaud S, Bolduc S, Pouliot F. Exosomes induce fibroblast differentiation into cancer-associated fibroblasts through TGFb signaling. *Mol Cancer Res*. 2018;16(7):1196-1204. doi:10.1158/1541-7786.MCR-17-0784

155. Paggetti J, Haderk F, Seiffert M, et al. Exosomes released by chronic lymphocytic leukemia cells induce the transition of stromal cells into cancer-associated fibroblasts. *Blood*. 2015;126(9):1106-1117. doi:10.1182/blood-2014-12-618025

156. Psaila B, Lyden D. The metastatic niche: adapting the foreign soil. *Nat Rev Cancer*. 2009;9:285-293.

157. Hood JL, San Roman S, Wickline SA. Exosomes released by melanoma cells prepare sentinel lymph nodes for tumor metastasis. *Cancer Res*. 2011;71(11):3792-3801. doi:10.1158/0008-5472.CAN-10-4455

158. Costa-Silva B, Aiello NM, Ocean AJ, et al. Pancreatic cancer exosomes initiate pre-metastatic niche formation in the liver. *Nat Cell Biol*. 2015;17(6):816-826. doi:10.1038/ncb3169

159. Kaplan RN, Riba RD, Zacharoulis S, et al. VEGFR1-positive haematopoietic bone marrow progenitors initiate the pre-metastatic niche. *Nature*. 2005;438(8):820-827. doi:10.1038/nature04186

160. Wang Y, Ding Y, Guo N, Wang S. MDSCs: Key criminals of tumor pre-metastatic niche formation. *Front Immunol*. 2019;10(172). doi:10.3389/fimmu.2019.00172

161. Margaret Lee YT. Patterns of metastasis and natural courses of breast carcinoma. *Cancer Metastasis Rev*. 1985;4(2):153-172. doi:10.1007/BF00050693

162. Bubendorf L, Schöpfer A, Wagner U, et al. Metastatic patterns of prostate cancer: An autopsy study of 1,589 patients. *Hum Pathol*. 2000;31(5):578-583. doi:10.1053/hp.2000.6698

163. Zhao L, Ma X, Yu J. Exosomes and organ-specific metastasis. *Mol Ther - Methods Clin Dev*. 2021;22(95):133-147. doi:10.1016/j.omtm.2021.05.016

164. Hoshino A, Costa-Silva B, Shen TL, et al. Tumour exosome integrins determine organotropic metastasis. *Nature*. 2015;527:329-335. doi:10.1038/nature15756

165. Hamidi H, Ivaska J. Every step of the way: integrins in cancer progression and metastasis. *Nat Rev Cancer*. 2018;18(9):533-548. doi:10.1038/s41568-018-0038-z

166. Bianconi D, Unseld M, Prager GW. Integrins in the spotlight of cancer. *Int J Mol Sci*. 2016;17(12). doi:10.3390/ijms17122037

167. Mitra SK, Schlaepfer DD. Integrin-regulated FAK-Src signaling in normal and cancer cells. *Curr Opin Cell Biol*. 2006;18(5):516-523. doi:10.1016/j.ceb.2006.08.011

168. Su CY, Li JQ, Zhang LL, et al. The Biological Functions and Clinical Applications of Integrins in Cancers. *Front Pharmacol*. 2020;11:579068. doi:10.3389/fphar.2020.579068

169. Desgrosellier JS, Cheresh DA. Integrins in cancer: Biological implications and therapeutic opportunities. *Nat Rev Cancer*. 2010;10:9-22. doi:10.1038/nrc2748

170. Yousefi H, Vatanmakanian M, Mahdiannasser M, et al. Understanding the role of integrins in breast cancer invasion, metastasis, angiogenesis, and drug resistance. *Oncogene*. 2021;40:1043-1063. doi:10.1038/s41388-020-01588-2

171. Belkin AM, Stepp MA. Integrins as receptors for laminins. *Microsc Res Tech*. 2000;51(3):280-301. doi:10.1002/1097-0029(20001101)51:3<280::AID-JEMT7>3.0.CO;2-O

172. Krishn SR, Singh A, Bowler N, et al. Prostate cancer sheds the αvβ3 integrin in vivo through exosomes. *Matrix Biol*. 2019;77:41-57. doi:10.1016/j.matbio.2018.08.004

173. Tumbarello DA, Turner CE. High Affinity Interaction of Integrin α4β1 (VLA-4) and Vascular Cell Adhesion Molecule 1 (VCAM-1) Enhances Migration of Human Melanoma Cells Across Activated Endothelial Cell Layers. *J Cell Physiol*. 2006;211(3)(May):736-747. doi:10.1002/JCP

174. Garmy-Susini B, Avraamides CJ, Desgrosellier JS, et al. PI3Ka activates integrin α4β1 to establish a metastatic niche in lymph nodes. *Proc Natl Acad Sci U S A*. 2013;110(22):9042-9047. doi:10.1073/pnas.1219603110

175. Steeg PS. Targeting metastasis. *Nat Rev Cancer*. 2016;16(4):201-218. doi:10.1038/nrc.2016.25

176. Lambert AW, Pattabiraman DR, Weinberg RA. Emerging Biological Principles of Metastasis. *Cell*. 2017;168(4):670-691. doi:10.1016/j.cell.2016.11.037

177. Yates LR, Gerstung M, Knappskog S, et al. Subclonal diversification of primary breast cancer revealed by multiregion sequencing. *Nat Med*. 2015;21(7):751-759. doi:10.1038/nm.3886

178. Anderson RL, Balasas T, Callaghan J, et al. A framework for the development of effective anti-metastatic agents. *Nat Rev Clin Oncol*. 2019;16(3):185-204. doi:10.1038/s41571-018-0134-8

179. Caswell DR, Swanton C. The role of tumour heterogeneity and clonal cooperativity in metastasis, immune evasion and clinical outcome. *BMC Med*. 2017;15(1):1-9. doi:10.1186/s12916-017-0900-y

180. Fidler IJ, Kripke ML. The challenge of targeting metastasis. *Cancer Metastasis Rev*. 2015;34(4):635-641. doi:10.1007/s10555-015-9586-9

181. Winer A, Adams S, Mignatti P. Matrix metalloproteinase inhibitors in cancer therapy: Turning past failures into future successes. *Mol Cancer Ther*. 2018;17(6):1147-1155. doi:10.1158/1535-7163.MCT-17-0646

182. Chinot OL. Cilengitide in glioblastoma: When did it fail? *Lancet Oncol*. 2014;15(10):1044-1045. doi:10.1016/S1470-2045(14)70403-6

183. Brown JE, Coleman RE. Denosumab in patients with cancer-a surgical strike against the osteoclast. *Nat Rev Clin Oncol*. 2012;9(2):110-118. doi:10.1038/nrclinonc.2011.197

184. Castellano D, Sepulveda JM, García-Escobar I, Rodriguez-Antolín A, Sundlöv A, Cortes-Funes H. The Role of RANK-Ligand Inhibition in Cancer: The Story of Denosumab. *Oncologist*. 2011;16(2):136-145. doi:10.1634/theoncologist.2010-0154

185. Smith MR, Saad F, Coleman R, et al. Denosumab and bone-metastasis-free survival in men with castration-resistant prostate cancer: Results of a phase 3, randomised, placebo-controlled trial. *Lancet*. 2012;379(9810):39-46. doi:10.1016/S0140-6736(11)61226-9

186. Gül G, Sendur MAN, Aksoy S, Sever AR, Altundag K. A comprehensive review of denosumab for bone metastasis in patients with solid tumors. *Curr Med Res Opin*. 2016;32(1):133-145. doi:10.1185/03007995.2015.1105795

187. Casas A, Llombart A, Martín M. Denosumab for the treatment of bone metastases in advanced breast cancer. *Breast*. 2013;22(5):585-592. doi:10.1016/j.breast.2013.05.007

188. Meirson T, Gil-Henn H, Samson AO. Invasion and metastasis: the elusive hallmark of cancer. *Oncogene*. 2020;39(9):2024-2026. doi:10.1038/s41388-019-1110-1

189. Verdine GL, Walensky LD. The challenge of drugging undruggable targets in cancer: Lessons learned from targeting BCL-2 family members. *Clin Cancer Res*. 2007;13(24):7264-7270. doi:10.1158/1078-0432.CCR-07-2184

190. Dang C V., Reddy EP, Shokat KM, Soucek L. Drugging the "undruggable" cancer targets. *Nat Rev Cancer*. 2017;17(8):502-508. doi:10.1038/nrc.2017.36

191. Kole R, Krainer AR, Altman S. RNA therapeutics: Beyond RNA interference and antisense oligonucleotides. *Nat Rev Drug Discov*. 2012;11(2):125-140. doi:10.1038/nrd3625

192. Kulkarni JA, Witzigmann D, Thomson SB, et al. The current landscape of nucleic acid therapeutics. *Nat Nanotechnol*. 2021;16(6):630-643. doi:10.1038/s41565-021-00898-0

193. Baden LR, El Sahly HM, Essink B, et al. Efficacy and Safety of the mRNA-1273 SARS-CoV-2 Vaccine. *N Engl J Med*. 2021;384(5):403-416. doi:10.1056/nejmoa2035389

194. Polack FP, Thomas SJ, Kitchin N, et al. Safety and Efficacy of the BNT162b2 mRNA Covid-19 Vaccine. *N Engl J Med*. 2020;383(27):2603-2615. doi:10.1056/nejmoa2034577

195. Damase TR, Sukhovershin R, Boada C, Taraballi F, Pettigrew RI, Cooke JP. The Limitless Future of RNA Therapeutics. *Front Bioeng Biotechnol*. 2021;9:628137. doi:10.3389/fbioe.2021.628137

196. Dias N, Stein CA. Antisense oligonucleotides: Basic concepts and mechanisms. *Mol Cancer Ther*. 2002;1(5):347-355.

197. Scoles DR, Minikel E V., Pulst SM. Antisense oligonucleotides: A primer. *Neurol Genet*. 2019;15(2):e323. doi:10.1212/NXG.0000000000000323

198. Rinaldi C, Wood MJA. Antisense oligonucleotides: The next frontier for treatment of neurological disorders. *Nat Rev Neurol*. 2018;14(1):9-22. doi:10.1038/nrneurol.2017.148

199. Karaki S, Paris C, Rocchi P. Antisense Oligonucleotides, A Novel Developing Targeting Therapy. In: *Antisense Therapy*. ; 2019:4-5. http://dx.doi.org/10.5772/intechopen.82105

200. Shen X, Corey DR. Chemistry, mechanism and clinical status of antisense oligonucleotides and duplex RNAs. *Nucleic Acids Res*. 2018;46(4):1584-1600. doi:10.1093/nar/gkx1239

201. Crooke ST, Witztum JL, Bennett CF, Baker BF. RNA-Targeted Therapeutics. *Cell Metab*. 2018;27(4):714-739. doi:10.1016/j.cmet.2018.03.004

202. Xiong H, Veedu RN, Diermeier SD. Recent advances in oligonucleotide therapeutics in oncology. *Int J Mol Sci*. 2021;22(7):3295. doi:10.3390/ijms22073295

203. Roberts TC, Langer R, Wood MJA. Advances in oligonucleotide drug delivery. *Nat Rev Drug Discov*. 2020;19(10):673-694. doi:10.1038/s41573-020-0075-7

204. Bennett CF. Therapeutic antisense oligonucleotides are coming of age. *Annu Rev Med*. 2019;70:307-321. doi:10.1146/annurev-med-041217-010829

205. Adams D, Koike H, Slama M, Coelho T. Hereditary transthyretin amyloidosis: a model of medical progress for a fatal disease. *Nat Rev Neurol*. 2019;15(7):387-404. doi:10.1038/s41582-019-0210-4

206. Benson MD, Waddington-Cruz M, Berk JL, et al. Inotersen Treatment for Patients with Hereditary Transthyretin Amyloidosis. *N Engl J Med*. 2018;379(1):22-31. doi:10.1056/nejmoa1716793

207. Brad Wan W, Seth PP. The Medicinal Chemistry of Therapeutic Oligonucleotides. *J Med Chem*. 2016;59(21):9645-9667. doi:10.1021/acs.jmedchem.6b00551

208. Dowdy SF. Overcoming cellular barriers for RNA therapeutics. *Nat Biotechnol*. 2017;35(3):222-229. doi:10.1038/nbt.3802

209. Bost JP, Barriga H, Holme MN, et al. Delivery of Oligonucleotide Therapeutics:

Chemical Modifications, Lipid Nanoparticles, and Extracellular Vesicles. *ACS Nano*. 2021;15(9):13993-14021. doi:10.1021/acsnano.1c05099

210. Fumoto S, Yamamoto T, Okami K, et al. Understanding in vivo fate of nucleic acid and gene medicines for the rational design of drugs. *Pharmaceutics*. 2021;13(2):1-35. doi:10.3390/pharmaceutics13020159
211. Geary RS, Norris D, Yu R, Bennett CF. Pharmacokinetics, biodistribution and cell uptake of antisense oligonucleotides. *Adv Drug Deliv Rev*. 2015;87:46-51. doi:10.1016/j.addr.2015.01.008
212. Sahay G, Querbes W, Alabi C, et al. Efficiency of siRNA delivery by lipid nanoparticles is limited by endocytic recycling. *Nat Biotechnol*. 2013;31(7):653-658. doi:10.1038/nbt.2614
213. Hawner M, Ducho C. Cellular Targeting of Oligonucleotides by Conjugation with Small Molecules. *Molecules*. 2020;25:5963. doi:10.3390/molecules25245963
214. Kilanowska A, Studzi ska S. In vivo and in vitro studies of antisense oligonucleotides - a review. *RSC Adv*. 2020;10(57):34501-34516. doi:10.1039/d0ra04978f
215. Manzari MT, Shamay Y, Kiguchi H, Rosen N, Scaltriti M, Heller DA. Targeted drug delivery strategies for precision medicines. *Nat Rev Mater*. 2021;6:351-370. doi:10.1038/s41578-020-00269-6
216. Kaczmarek JC, Kowalski PS, Anderson DG. Advances in the delivery of RNA therapeutics: From concept to clinical reality. *Genome Med*. 2017;9:60. doi:10.1186/s13073-017-0450-0
217. Dreaden EC, Alkilany AM, Huang X, Murphy CJ, El-Sayed MA. The golden age: Gold nanoparticles for biomedicine. *Chem Soc Rev*. 2012;41(7):2740-2779. doi:10.1039/c1cs15237h
218. Roma-Rodrigues C, Raposo LR, Cabral R, Paradinha F, Baptista P V., Fernandes AR. Tumor microenvironment modulation via gold nanoparticles targeting malicious exosomes: Implications for cancer diagnostics and therapy. *Int J Mol Sci*. 2017;18(1):162. doi:10.3390/ijms18010162
219. Riehemann K, Schneider SW, Luger TA, Godin B, Ferrari M, Fuchs H. Nanomedicine — Challenge and Perspectives. *Angew Chem Int Ed*. 2009;48:872-897. doi:10.1002/anie.200802585
220. Pelaz B, Alexiou C, Alvarez-puebla RA, et al. Diverse Applications of Nanomedicine. *ACS Nano*. 2017;11:2313-2381. doi:10.1021/acsnano.6b06040
221. Chan WCW, Ph D. Nanomedicine. *N Engl J Med*. 2010;363:25.
222. Shi J, Kantoff PW, Wooster R, Farokhzad OC. Cancer nanomedicine : progress , challenges and opportunities. *Nat Rev Cancer*. 2017;17:20-37. doi:10.1038/nrc.2016.108
223. Murphy CJ, Gole AM, Stone JW, et al. Gold Nanoparticles in Biology: Beyond Toxicity to Cellular Imaging. *Acc Chem Res*. 2008;41(12):1721-1730.
224. Giljohann DA, Seferos DS, Daniel WL, Massich MD, Patel PC, Mirkin CA. Gold nanoparticles for biology and medicine. *Angew Chemie - Int Ed*. 2010;49(19):3280-3294. doi:10.1002/anie.200904359
225. Khan I, Saeed K, Khan I. Nanoparticles: Properties, applications and toxicities. *Arab J Chem*. 2019;12(7):908-931. doi:10.1016/j.arabjc.2017.05.011
226. Boisselier E, Astruc D. Gold nanoparticles in nanomedicine: preparations, imaging, diagnostics, therapies and toxicity. *Chem Soc Rev*. 2009;38(6):1759-1782. doi:10.1039/b806051g

227. Lim ZZJ, Li JEJ, Ng CT, Yung LYL, Bay BH. Gold nanoparticles in cancer therapy. *Acta Pharmacol Sin*. 2011;32(8):983-990. doi:10.1038/aps.2011.82

228. Sztandera K, Gorzkiewicz M, Klajnert-Maculewicz B. Gold Nanoparticles in Cancer Treatment. *Mol Pharm*. 2019;16(1):1-23. doi:10.1021/acs.molpharmaceut.8b00810

229. Siddique S, Chow JCL. Gold nanoparticles for drug delivery and cancer therapy. *Appl Sci*. 2020;10(11). doi:10.3390/app10113824

230. Bansal SA, Kumar V, Karimi J, Singh AP, Kumar S. Role of gold nanoparticles in advanced biomedical applications. *Nanoscale Adv*. 2020;2(9):3764-3787. doi:10.1039/d0na00472c

231. Online V. Biological applications of gold nanoparticles. *Chem Soc Rev*. 2008;37(9):1909-1930. http://www.ncbi.nlm.nih.gov/pubmed/18762839

232. Pan Y, Neuss S, Leifert A, et al. Size-dependent cytotoxicity of gold nanoparticles. *Small*. 2007;3(11):1941-1949. doi:10.1002/smll.200700378

233. Conde J, Larguinho M, Cordeiro A, et al. Gold-nanobeacons for gene therapy: Evaluation of genotoxicity, cell toxicity and proteome profiling analysis. *Nanotoxicology*. 2014;8(5):521-532. doi:10.3109/17435390.2013.802821

234. Carnovale C, Bryant G, Shukla R, Bansal V. Identifying Trends in Gold Nanoparticle Toxicity and Uptake: Size, Shape, Capping Ligand, and Biological Corona. *ACS Omega*. 2019;4(1):242-256. doi:10.1021/acsomega.8b03227

235. Connor EE, Mwamuka J, Gole A, Murphy CJ, Wyatt MD. Gold nanoparticles are taken up by human cells but do not cause acute cytotoxicity. *Small*. 2005;1(3):325-327. doi:10.1002/smll.200400093

236. Lee E, Jeon H, Lee M, et al. Molecular origin of AuNPs-induced cytotoxicity and mechanistic study. *Sci Rep*. 2019;9(1):1-13. doi:10.1038/s41598-019-39579-3

237. Ghosh P, Han G, De M, Kim CK, Rotello VM. Gold nanoparticles in delivery applications. *Adv Drug Deliv Rev*. 2008;60(11):1307-1315. doi:10.1016/j.addr.2008.03.016

238. Rahme K, Nolan MT, Doody T, et al. Highly stable PEGylated gold nanoparticles in water: Applications in biology and catalysis. *RSC Adv*. 2013;3(43):21016-21024. doi:10.1039/c3ra41873a

239. Suka JS, Xua Q, Kima N, Hanesa J, EnsignaHosein LM. PEGylation as a strategy for improving nanoparticle-based drug and gene delivery. *Physiol Behav*. 2017;176(3):139-148. doi:10.1016/j.addr.2015.09.012.PEGylation

240. Manson J, Kumar D, Meenan BJ, Dixon D. Polyethylene glycol functionalized gold nanoparticles: The influence of capping density on stability in various media. *Gold Bull*. 2011;44(2):99-105. doi:10.1007/s13404-011-0015-8

241. Zhang J, Mou L, Jiang X. Surface chemistry of gold nanoparticles for health-related applications. *Chem Sci*. 2020;11(4):923-936. doi:10.1039/c9sc06497d

242. Verma A, Stellacci F. Effect of surface properties on nanoparticle-cell interactions. *Small*. 2010;6(1):12-21. doi:10.1002/smll.200901158

243. Amina SJ, Guo B. A review on the synthesis and functionalization of gold nanoparticles as a drug delivery vehicle. *Int J Nanomedicine*. 2020;15:9823-9857. doi:10.2147/IJN.S279094

244. Ferreira D, Fontinha D, Martins C, Pires D, Fernandes AR, Baptista P V. Gold nanoparticles for vectorization of nucleic acids for cancer therapeutics. *Molecules*. 2020;25:3489. doi:10.3390/molecules25153489

245. Ding Y, Jiang Z, Saha K, et al. Gold nanoparticles for nucleic acid delivery. *Mol Ther*. 2014;22(6):1075-1083. doi:10.1038/mt.2014.30

246. Rosi NL, Giljohann DA, Thaxton CS, Lytton-Jean AKR, Han MS, Mirkin CA. Oligonucleotide-modified gold nanoparticles for infracellular gene regulation. *Science*. 2006;312:1027-1030. doi:10.1126/science.1125559

247. Hurst SJ, Lytton-Jean AKR, Mirkin CA. Maximizing DNA Loading on a Range of Gold Nanoparticle Sizes. *Anal Chem*. 2006;78(24):8313-8318. doi:10.1021/ac0613582.Maximizing

248. Peer D, Karp JM, Hong S, Farokhzad OC, Margalit R, Langer R. Nanocarriers as an emerging platform for cancer therapy. *Nat Nanotechnol*. 2007;2:751-760. doi:10.1038/nnano.2007.387

249. Rosenblum D, Joshi N, Tao W, Karp JM, Peer D. Progress and challenges towards targeted delivery of cancer therapeutics. *Nat Commun*. 2018;9:1410. doi:10.1038/s41467-018-03705-y

250. Golombek SK, May JN, Theek B, et al. Tumor targeting via EPR: Strategies to enhance patient responses. *Adv Drug Deliv Rev*. 2018;130:17-38. doi:10.1016/j.addr.2018.07.007

251. Smith SA, Selby LI, Johnston APR, Such GK. The Endosomal Escape of Nanoparticles: Toward More Efficient Cellular Delivery. *Bioconjug Chem*. 2019;30(2):263-272. doi:10.1021/acs.bioconjchem.8b00732

252. Oliveira H, Roma-Rodrigues C, Santos A, et al. GLUT1 and GLUT3 involvement in anthocyanin gastric transport- Nanobased targeted approach. *Sci Rep*. 2019;9:789. doi:10.1038/s41598-018-37283-2

253. Conde J, Rosa J, de la Fuente JM, Baptista P V. Gold-nanobeacons for simultaneous gene specific silencing and intracellular tracking of the silencing events. *Biomaterials*. 2013;34(10):2516-2523. doi:10.1016/j.biomaterials.2012.12.015

254. Bao C, Conde J, Curtin J, Artzi N, Tian F, Cui D. Bioresponsive antisense DNA gold nanobeacons as a hybrid in vivo theranostics platform for the inhibition of cancer cells and metastasis. *Sci Rep*. 2015;5:12297. doi:10.1038/srep12297

255. Roma-Rodrigues C, Pereira F, Alves de Matos AP, Fernandes M, Baptista P V., Fernandes AR. Smuggling gold nanoparticles across cell types – A new role for exosomes in gene silencing. *Nanomedicine Nanotechnology, Biol Med*. 2017;13(4):1389-1398. doi:10.1016/j.nano.2017.01.013

256. Conde J, Ambrosone A, Sanz V, et al. Design of multifunctional gold nanoparticles for in vitro and in vivo gene silencing. *ACS Nano*. 2012;6(9):8316-8324. doi:10.1021/nn3030223

257. Kumthekar P, Ko CH, Paunesku T, et al. A first-in-human phase 0 clinical study of RNA interference-based spherical nucleic acids in patients with recurrent glioblastoma. *Sci Transl Med*. 2021;13(584):1-31. doi:10.1126/scitranslmed.abb3945

258. Zadeh JN, Steenberg CD, Bois JS, et al. NUPACK: analysis and design of nucleic acid systems. *J Comput Chem*. 2011;32(1):170-173. doi:10.1002/jcc.21596

259. Gruber A, Lorenz R, Bernhart S, Neuböck R, Hofacker I. The Vienna RNA Websuite. *Nucleic Acids Res*. 2008;36:w70-w74. doi:10.1093/nar/gkn188

260. Turkevich J, Stevenson PC, Hillier J. A study of the nucleation and growth processes in the synthesis of colloidal gold. *Discuss Faraday Soc*. 1951;11:55-75.

261. Lee PC, Meisel D. Adsorption and surface-enhanced Raman of dyes on silver and gold sols. *J Phys Chem*. 1982;86(17):3391-3395. doi:10.1021/j100214a025

262. Conde J. Cancer Theranostics: Multifunctional Gold Nanoparticles for Diagnostics and Therapy. 2013. PhD thesis, Universidade Nova de Lisboa & Universidad de Zaragoza, Lisbon. http://run.unl.pt/handle/10362/10927

263. Hu T, Zhou R, Zhao Y, Wu G. Integrin α6/Akt/Erk signaling is essential for human breast cancer resistance to radiotherapy. *Sci Rep*. 2016;6(August):1-10. doi:10.1038/srep33376

264. Schmittgen TD, Livak KJ. Analyzing real-time PCR data by the comparative CT method. *Nat Protoc*. 2008;3(6):1101-1108. doi:10.1038/nprot.2008.73

265. Schneider CA, Rasband WS, Eliceiri KW. NIH Image to ImageJ: 25 years of image analysis. *Nat Methods*. 2012;9(7):671-675. doi:10.1038/nmeth.2089

266. Biochemistry C. α6-Integrin Is Required for the Adhesion and Vasculogenic Potential of Hemangioma Stem Cells. *Stem Cells*. 2014;32:684-693.

267. Ferreira Golbert DC, Correa-de-Santana E, Ribeiro-Alves M, de Vasconcelos ATR, Savino W. ITGA6 gene silencing by RNA interference modulates the expression of a large number of cell migration-related genes in human thymic epithelial cells. *BMC Genomics*. 2013;14(Suppl 6):S3. doi:10.1186/1471-2164-14-S6-S3

268. Golbert DCF, Santana-Van-Vliet E, Ribeiro-Alves M, et al. Small interference ITGA6 gene targeting in the human thymic epithelium differentially regulates the expression of immunological synapse-related genes. *Cell Adhes Migr*. 2018;12(2):152-167. doi:10.1080/19336918.2017.1327513

269. Vinhas R. Gold nanoparticles for nanotheranostics in leukemia – Addressing Chronic Myeloid Leukemia. 2018. PhD thesis, Universidade Nova de Lisboa, Lisbon. http://hdl.handle.net/10362/37531

270. Jokerst J V, Lobovkina T, Zare RN, Gambhir SS. Nanoparticle PEGylation for imaging and therapy. *Nanomedicine (Lond)*. 2011;6(4):715-728. doi:10.2217/nnm.11.19.Nanoparticle

271. Pereira FSR de F. Blocking tumor exosome release using nanovectorization systems. 2015. MSc thesis, Universidade Nova de Lisboa, Lisbon. http://hdl.handle.net/10362/16193

272. Sanz V, Conde J, Hernández Y, Baptista P V., Ibarra MR, De La Fuente JM. Effect of PEG biofunctional spacers and TAT peptide on dsRNA loading on gold nanoparticles. *J Nanoparticle Res*. 2012;14:917. doi:10.1007/s11051-012-0917-2

273. Jia S, Bian C, Sun J, Tong J, Xia S. A wavelength-modulated localized surface plasmon resonance (LSPR) optical fiber sensor for sensitive detection of mercury(II) ion by gold nanoparticles-DNA conjugates. *Biosens Bioelectron*. 2018;114:15-21. doi:10.1016/j.bios.2018.05.004

274. Sadalage PS, Patil R V., Havaldar D V., Gavade SS, Santos AC, Pawar KD. Optimally biosynthesized, PEGylated gold nanoparticles functionalized with quercetin and camptothecin enhance potential anti-inflammatory, anti-cancer and anti-angiogenic activities. *J Nanobiotechnology*. 2021;19:84. doi:10.1186/s12951-021-00836-1

275. Wang R, Bowling I, Liu W. Cost effective surface functionalization of gold nanoparticles with a mixed DNA and PEG monolayer for nanotechnology applications. *RSC Adv*. 2017;7(7):3676-3679. doi:10.1039/C6RA26791B

276. Wu R, Peng H, Zhu JJ, Jiang LP, Liu J. Attaching DNA to Gold Nanoparticles With a Protein Corona. *Front Chem*. 2020;8:121. doi:10.3389/fchem.2020.00121

277. Vinhas R, Fernandes AR, Baptista P V. Gold Nanoparticles for BCR-ABL1 Gene

Silencing: Improving Tyrosine Kinase Inhibitor Efficacy in Chronic Myeloid Leukemia. *Mol Ther - Nucleic Acids*. 2017;7:408-416. doi:10.1016/j.omtn.2017.05.003

278. Owczarzy R, Tataurov A V., Wu Y, et al. IDT SciTools: a suite for analysis and design of nucleic acid oligomers. *Nucleic Acids Res*. 2008;36:W163–W169. doi:10.1093/nar/gkn198

279. Ye J, Coulouris G, Zaretskaya I, Cutcutache I, Rozen S, Madden TL. Primer-BLAST: A tool to design target-specific primers for polymerase chain reaction. *Bioinformatics*. 2012;13:134. doi:10.1186/1471-2105-13-134

280. Farrell JR. RE. *RNA Methodologies. Laboratory Guide for Isolation and Characterization.* Fifth Edit. Academic Press; 2017.

281. Moreno-Layseca P, Icha J, Hamidi H, Ivaska J. Integrin trafficking in cells and tissues. *Nat Cell Biol*. 2019;21(2):122-132. doi:10.1038/s41556-018-0223-z

282. López-Ceballos P, DonajíHerrera-Reyes A, Coombs D, Tanentzapf G. In vivo regulation of integrin turnover by outside-in activation. *J Cell Sci*. 2016;129(15):2912-2924. doi:10.1242/jcs.190256

283. Margadant C, Monsuur HN, Norman JC, Sonnenberg A. Mechanisms of integrin activation and trafficking. *Curr Opin Cell Biol*. 2011;23(5):607-614. doi:10.1016/j.ceb.2011.08.005

284. Bachmann M, Kukkurainen S, Hytönen VP, Wehrle-Haller B. Cell adhesion by integrins. *Physiol Rev*. 2019;99(4):1655-1699. doi:10.1152/physrev.00036.2018